JOURNAL OF BUILDING PHYSICS

Research Paper

Journal of Building Physics
2022, Vol. 45(5) 675–720

DOI: 10.1177/17442591211045418
journals.sagepub.com/home/jen
SAGE

Adaptive opaque façades and their potential to reduce thermal energy use in residential buildings: A simulation-based evaluation

Miren Juaristi[1], Fabio Favoino[2], Tomás Gómez-Acebo[3] and Aurora Monge-Barrio[1]

Abstract

Adaptive façades are a promising choice to achieve comfortable low-energy buildings. Their effective performance is highly dependent on the local boundary conditions of each application and on the way the dynamic properties are controlled. The evaluation of whole building performance through building performance simulation can be useful to understand the potential of different Adaptive opaque façades (AOF) in a specific context. This paper evaluates through dynamic simulations promising design solutions of AOF for a residential building use in six different climates. It quantifies the total delivered thermal energy of 15 typologies of AOFs which consist of alternative adaptation strategies: (i) variation of solar absorptance of the cladding, (ii) variation of the convective heat transfer of air cavities and (iii) adaptive insulation strategies. For the first time, it also quantifies the performance of AOF which combine more than one adaptation strategy. The results show that the variation of the heat transfer by means of Adaptive Insulation components has the most significant impact on the reduction of the thermal energy use. The variation of the solar absorptance has also a significant positive impact

[1]School of Architecture, Universidad de Navarra, Pamplona, Spain
[2]Department of Energy, Politecnico di Torino, Torino, Italy
[3]TECNUN School of Engineers, Universidad de Navarra, San Sebastián, Spain

Corresponding author:
Miren Juaristi, School of Architecture, University of Navarra, Campus Universitario, Pamplona, Navarra 31009, Spain.
Email: mjuaristi@alumni.unav.es

when reducing heating consumption, but only if this adaptation strategy is actively controlled and combined with Adaptive Insulation components.

Keywords
Adaptive heat transfer, adaptive insulation, switchable coatings, kinetic claddings, building performance simulation, thermal performance

Introduction

A notable part of research in the built environment is focused on the development of promising building technologies that can improve the energy performance and users' comfort, motivated by the urgent need of achieving low-energy buildings which can contribute to the reduction of greenhouse gas emissions (Yılmaz and Yılmaz, 2021). Adaptive Facades are among the many concepts with high potential (Aschehoug et al., 2008). Their main feature is to embed materials, components and systems which allow '…to repeatedly and reversibly change some of its functions, features or behaviour over time in response to changing performance requirements and variable boundary conditions and does this with the aim of improving overall building performance' (Loonen et al., 2013). There are already several built examples of Adaptive Facades and so far, their application for automated management of solar gains and daylight, such as operable solar shading devices and smart glazing are the most developed and studied (Aelenei et al., 2018). A less explored Adaptive Façade typology is Adaptive opaque façades (AOF), which integrate into the opaque part of the facade adaptive technologies and materials aimed at managing and controlling the heat transfer between the outdoor and the indoor environment, by means of different strategies (which are reviewed in Section 1.1). AOF can dissipate thermal energy when indoor spaces are overheated and can also contribute to reduce heating demand by obtaining heat gains from the outdoor medium when the incident solar radiation is high enough. Their integration in residential buildings seems especially promising, as they have larger opaque façade areas than other building uses and the heating and cooling energy are the most used energy type in residential buildings (Ürge-Vorsatz et al., 2015). Unlike natural ventilation strategies, which might be an effective strategy to dissipate internal heat gains, in suitable climates and building uses AOF can both reduce cooling needs and heating demand in a substantial way (Jin et al., 2017). Besides, AOF can also be useful design option to reduce cooling demand in built environments with high environmental noise levels, where promoting natural ventilation might be an issue (Koenders et al., 2018). There are few research studies regarding different types of AOF and most of them are still at a conceptual and/or for the simplest typologies, at numerical evaluation level (Juaristi et al., 2018a), although in the coming years different commercial technologies could become available (Cui and Overend, 2019; Koenders et al., 2018; Pflug et al., 2015).

The market uptake of AOF however could be limited by (i) the progress in specific product development, aiming at finding a good compromise among performance, durability and cost, but also by (ii) the challenges designers could face to control the design, construction process and operation of dynamic building envelope technologies (Attia et al., 2018). In fact, as a result of their controllable physical properties, traditional facade design approaches might not be directly applicable for adaptive building envelope systems (Bianco et al., 2018). The opportunity presented by such dynamic façade systems in improving whole building performance will highly depend on the way these technologies are integrated into the overall building strategy, the range of their dynamic properties and their control logics (whether passively or actively controlled) compared to the dynamicity of local boundary conditions (both outdoor climate and variability of internal conditions). For these reasons, unlike traditional envelope elements, adaptive envelope systems cannot be simplistically compared by using performance metrics, which are derived for non-dynamic components considering steady-state boundary conditions (such as U-value, Admittance values, etc.), even though these metrics could be easily calculated directly from physical characteristics of the materials. In this context, building simulations can be a useful tool to transform these challenges into an opportunity to inform design decisions for adaptive building envelope components, as they can help designers to understand how the adaptive façade solution is behaving under different boundary conditions and could affect whole building performance indicators (such as energy use and occupant comfort; Favoino et al., 2018; Loonen et al., 2014).

To date research efforts have focused on evaluating the performance of specific adaptive façade technologies and systems which include only specific dynamic features (summarized in Table 1). These researches have been focused mostly on the product development and generally there is not a common design approach which could support early-stage design decisions of multi-layered adaptive opaque façade systems integrating one or more of adaptive façade strategies. Besides, they do not consider how the combination with other construction materials might modify the thermal performance of the façade.

Main technologies to build adaptive opaque facades

Adaptive Opaque Façade technologies could be classified by the strategy they use to manage the heat transfer between the outdoor and indoor environment through the façade element, which is summarized in Table 1.

Phase Change Materials (PCM) are one of the most studied technologies for their integration in Adaptive Opaque Facades (Juaristi et al., 2018a; Kuznik et al., 2011). PCMs store and release heat without any sensible temperature variation of the medium, with reversible phase change of freezing and melting. Unlike other building materials, the phase change takes place at built environment temperatures having a higher capacity to store latent heat. Over the last decade, researchers proposed simulation methods to predict their behaviour and performance (Fateh et al.,

Table 1. Main technologies to build Adaptive Opaque Facades and to achieve the heat transfer control within an opaque element.

Adaptive mechanism	Material/system dynamic characteristic		Technology	References
(i) Control of heat gains on the outer layer		(i.a) Variable solar absorptance of the cladding	(i.a) Thermochromics (TCH)*	(Chang et al., 2015; Garshasbi and Santamouris, 2019; Hu and Yu, 2019; Karlessi et al., 2009; Park and Krarti, 2016; Perez et al., 2018; Zheng et al., 2015)
			(i.a) Automated kinetic cladding (KC)*	(Juaristi et al., 2018b)
(ii) Control of heat transfer	(ii.a) Variable convective heat transfer	(ii.a.1) Variable air-flow exchange between outdoor conditions and ventilated air cavity	(ii.a.1) Controllable convective heat transfer of air cavities (AC)*	(Juaristi et al., 2018b)
		(ii.a.2) Variable air-flow exchange between outdoor and indoor environments	(ii.a.2) Parietodynamic insulation	(Baker, 2003; Dimoudi et al., 2004; Elsarrag et al., 2012; Imbabi, 2006)
			(ii.a.2) Permeodynamic insulation	(Elsarrag et al., 2012; Fantucci et al., 2015; Isaia et al., 2019)
	(ii.b) Variable convective/ conductive heat transfer	(ii.b) No air-flow exchange between adjacent construction elements	(ii.b) Adaptive Insulation components (AIS)*	(Berge et al., 2015; Berson et al., 1994; Clark et al., 2013; Cui and Overend, 2019; Favoino et al., 2017; Jin et al., 2017; Kimber et al., 2014; Koenders et al., 2018; Kvasnin, 2013; Park et al., 2015; Peeters and Dona, 2010; Pflug et al., 2015, 2017; Sunden et al., 2014; Varga et al., 2002)

(continued)

Table 1. Continued

Adaptive mechanism	Material/system dynamic characteristic	Technology	References
(iii) Thermal storage	(iii.a) Latent heat storage at ambient temperature (no sensible temperature variation)	(iii.a) Phase change materials (PCM)	(Arıcı et al., 2020; Cabeza et al., 2011; Carbonaro et al., 2015; Cascone et al., 2018; Castell et al., 2010; Fateh et al., 2018, 2019; Gassar and Yun, 2017; Goia et al., 2018; Izquierdo-Barrientos et al., 2012; Juaristi et al., 2018a; Kuznik et al., 2011; Li et al., 2019; UCLA, 2017)

*The simulation strategy applied in this paper supports the evaluation of these technologies.

2019; Gassar and Yun, 2017; Izquierdo-Barrientos et al., 2012) and built up experimental facilities to calibrate those models (Castell et al., 2010; Goia et al., 2018). These researches studied the possible integration of PCM in other building materials, analysed where PCM should be placed in multi-layered opaque façade systems and detected optimal melting point temperatures (Arıcı et al., 2020; Carbonaro et al., 2015; Cascone et al., 2018; Fateh et al., 2018; Li et al., 2019). These results might support designers when considering the application of such innovative technologies in multi-layered opaque facade systems, as they enable understanding how the latent heat can contribute to improve the thermal performance and they analysed and optimized different design parameters. Another good illustration of the scientific maturity of PCM is the development of a tool called Opaque 3.0 for early design stages. It determines the Average Daily Energy reduction when microencapsulated PCM is included in one of the layers of a composite surface (UCLA, 2017). Moreover, there are also several producers which commercialize façade elements containing PCM (Cabeza et al., 2011), while for the remainder AOF materials and systems all the technologies available are at a prototyping stage and no commercial product is still available.

Adaptive Insulation (AIS) concept refers in this paper to the construction components which have a variable convective and conduction heat transfer without any mass transfer (air-flow exchange) between adjacent construction elements, that is Close Loop Dynamic Insulation Systems (Koenders et al., 2018; Pflug et al., 2015), Multi-layered Movable Construction (Kimber et al., 2014), Variable Pressure Insulation panels and Variable Conductance Insulations (Berge et al., 2015; Berson et al., 1994), Bi-directional thermodiodes (Varga et al., 2002) and Carbon Nanotubes Suspensions (Sunden et al., 2014). However, adaptive heat transfer can also be achieved by managing the mass transfer between the indoor and outdoor environment, or between different layers of the opaque construction. A notable example of such adaptive behaviour are Parietodynamic and Permeodynamic walls, which take advantage of combined effects of solar radiation, wind, pressure and temperature differences between indoor and outdoor environments (Baker, 2003; Dimoudi et al., 2004; Elsarrag et al., 2012; Fantucci et al., 2015; Imbabi, 2006; Isaia et al., 2019). Research on Adaptive Insulations and adaptive heat transfer in opaque façade elements is an emerging field (Cui and Overend, 2019). Most of the studies analysed their potential contribution to reduce the thermal energy need by using different simulation strategies (Favoino et al., 2017; Jin et al., 2017; Koenders et al., 2018; Park et al., 2015; Pflug et al., 2017). There are only few concepts which were patented (Clark et al., 2013; Kvasnin, 2014; Peeters and Dona, 2010) and first experimental assessments and prototypes started recently to be built (Pflug et al., 2017). As there is a lack of experimental assessments, previous simulation studies, such as the ones carried out by Favoino et al. (Favoino et al., 2017), assumed thermal conductivity adaptation ranges of Adaptive Insulation based on literature review. However, sometimes they only found one indicator in the literature (i.e. only the U-value or only conductance (λ)) and when that happened, they calculated the missing λ or U value supposing a specific thickness of the insulation layer. So far, the lack of experimental assessment impedes to validate these values under different boundary conditions.

There are also different studies in Advanced and Switchable Coatings, which could enhance its application in AOF, as they can provide the variable solar absorptance of the cladding. However, so far, these studies tested the preparation of these coatings and their optical changes under different surface temperatures (Chang et al., 2015; Karlessi et al., 2009; Perez et al., 2018) and their application was mainly studied to reduce Heating Urban Island Effects (Garshasbi and Santamouris, 2019). Only few research studied the possible beneficial impact on the thermal energy performance when these coatings were applied in opaque facades (Zheng et al., 2015) and adaptive roof system (Hu and Yu, 2019; Park and Krarti, 2016).

Moreover, kinetic claddings with active control could also serve to achieve variable solar absorptance of the cladding (Juaristi et al., 2018b). This conceptual approach proposes an external cladding which is made by a material with a specific solar absorptance and the following layer is composed by another material with different thermal properties. Through the geometry change of the outer layer, the solar absorptance of the opaque façade changes. The adaptive geometry of the outer cladding can be achieved by integrating smart and multifunctional materials such as Shape Memory Alloys and Thermobimetals. These metals change their shape when they reach their operational temperature and come back to their original shape when they are cooled down. The shape change can also be actively controlled with a heat source induced by an electrical input.

At a conceptual level, shape changing façade elements were also proposed to exploit the variable air-flow exchange which might happen between the outdoor environment and the ventilated air cavity placed immediately after the cladding (Juaristi et al., 2018b). The modification of morphology of the ventilated air cavities (i.e. the opening degree of the external cladding joints and the upper and lower part of the air cavity) affects to the convective heat transfers. Thus, by controlling the morphology of the air cavity with kinetic elements, the heat losess can be enhanced/diminished. In this paper, the term ‘controllable convective heat transfer of air cavities’ refers to the above-named adaptive behaviour. The thermal characterization of controllable convective heat transfer of air cavities is a complex task, which needs experimental assessments and Computational Fluid Dynamics (CFD) simulations to understand in detail the impact of incident solar radiation and the resulting convective heat effects in the air cavities (Giancola et al., 2012; Ibañez-Puy et al., 2017; Sánchez et al., 2017). As far as the authors know, no research has been carried out to evaluate the thermal performance of kinetic claddings with active control and/or controllable convective heat transfer of air cavities. The lack of a simulation strategy impedes architects or façade engineers to understand the potential of applying AOF which include this kind of dynamic technologies.

Research scope and objectives

The main design goal of AOF is to reduce the thermal energy need (both heating and cooling) to maintain indoor thermal conditions, by managing the heat flow through the opaque part of the building envelope. The purpose of this paper is to assess the potential that 15 AOF typologies, have to reduce the thermal energy need with respect to a reference static opaque façade benchmark. To do so, a simulation strategy is developed, which for the first time is able to model synergies between different adaptive mechanisms within a single AOF system. Its scope is limited to the design and simulation of the opaque part of the facade with adaptive heat transfer behaviour that can be actively controlled, without any mass transfer between indoor and outdoor environment.

The study has been organized in the following way. Section 2 starts explaining the methodological framework for the simulations. Then, the overall simulation modelling strategy in Energy Plus is presented. Afterwards, in section 2.3, the different adaptation mechanisms and their specific simulation modelling methodology are presented. Considered adaptation ranges are also outlined based on the state of the art of the technologies. Section 2.4 establishes the simulation goals and the performance indicators to be evaluated, such as the reduction of energy need for heating and cooling. According to the specific climate and specific building under analysis, the Static Performance References (SPR) are established in section 2.5. Finally, the test case building model is described and the meaningful type of simulation outputs are identified. The third part of the paper presents the possible 15 AOF typologies and shows their simulation results. For the most promising AOF typologies, from the thermal energy use reduction perspective, the impact of decisive design decisions and the operational aspects are outlined.

Methodology

Simulation framework

The performed simulations followed the methodological framework proposed by Loonen et al. for the product development of innovative building envelope components (Loonen et al., 2014), which has been extended to include the particularities of Adaptive Opaque façade designs in the Building Performance Simulation. This is summarized in Figure 1 highlighting in grey the original steps of the framework and how it has been expanded for this specific case.

This research considered as a case study a representative space of a residential building located in six different climates. The purpose of applying the methodology in several locations was to study some potential differences in the obtainment of the design goal influenced by climatic conditions. Previous research (Juaristi et al., 2020) has established by the application of a Dynamic Climate Analysis that Athens (Greece), Almeria (Spain), Brisbane (Australia), Lisbon (Portugal), Auckland (New Zealand) and Tenerife (Spain) were among the 14 analysed climates providing a good distribution between Mediterranean and temperate

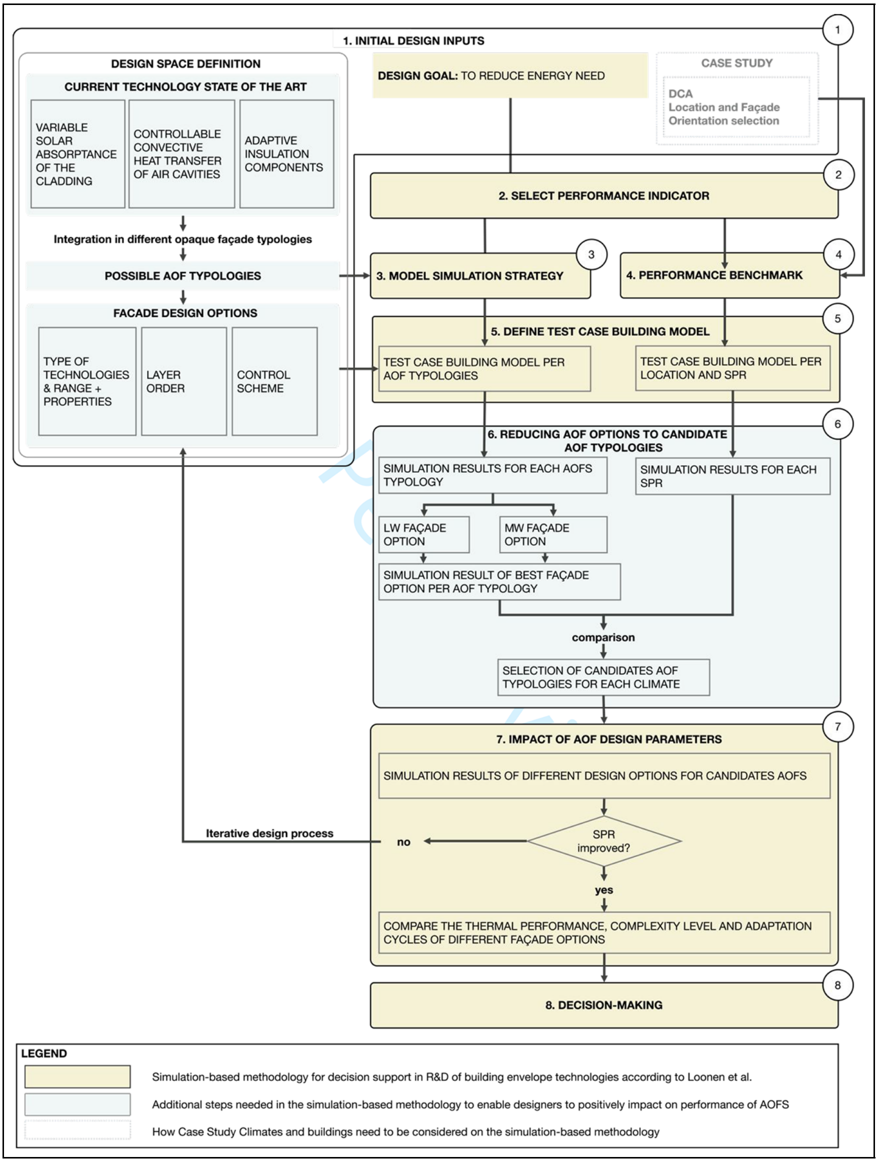

Figure 1. Simulation framework to detect the most promising Adaptive Opaque Facade typologies.

climates, the potential candidate locations to where AOFS could improve significantly the overall building energy use. Therefore, they were chosen to exemplify the application of the proposed approach. The West oriented façade was considered, as it was the most promising orientation to apply adaptive heat transfer façade responses, according to the cited research work (Juaristi et al., 2020). These climates are classified according to Köppen-Geiger Classification (Peel et al., 2007) as Mild Temperate Climates (Cfa), Hot-summer Mediterranean Climate (Csa), Warm-summer Mediterranean Climate (Csb) and Tropical savanna climate with dry-winter (Aw).

Besides, in order to narrow down the simulation space, these criteria was followed:

- When the finishing colour of the exterior (Ext) cladding or the insulation is static, the selected material for these layers will be the same as the ones applied in the Static Performance Reference (SPR).
- The insulation/AIS was placed in the outer side of the thermal mass of the building envelope, as previous researchers pointed out that is the best location to improve the thermal performance (Favoino et al., 2017).
- Adaptive Technologies with the highest adaptation ranges were selected among the different technological options which can vary the Solar Absorptance of claddings and Adaptive Insulation components, as higher adaptation ranges improve the overall thermal performance (Favoino et al., 2017).
- For Kinetic Claddings, as their adaptation range depends on the design and geometry, a second round of simulation will analyse the implications which this design decision has on the thermal performance when a certain geometrical configuration, with lower adaptation range, is applied.

Simulation model in Energy Plus

All the facade configurations were modelled within Energy Plus (EnergyPlus, 2020). Its conduction finite difference (CondFD) solution algorithm complements the CTF solution algorithm to simulate phase change materials or variable thermal conductivity, and it does so for zone time steps as short as 1 min. CondFD model calculates the temperatures of the building constructions both in the surfaces of each façade layer and in their interior (Int). To do so, each layer has (i) an interior surface node, (ii) (an/several) interior node(s), (iii) material interfaced nodes and (iv) external surface nodes. Because of the iteration scheme used for CondFD, the node enthalpies get updated each iteration. CondFD has another added benefit for the simulation-based design: the designer can know, at every time-step, the temperature of each façade layer. This information enables both the verification of the proper modelling and the employment of temperature-based sensors in the intermediate layers of the multi-layered opaque envelopes. This means that it is necessary to detect which nodes correspond to each surface layer in the simulation outputs. To do so, eliminating interior nodes is helpful. This can be achieved by increasing the Space Discretization constant. Table 2 summarizes the calculation parameters used to model the 15 AOF typologies. The only limitation of CondFD

Table 2. Simulation calculation parameters used for the modelling AOF typologies.

Simulation calculation parameters	Units	Value
Surface convection algorithm: inside		TARP
Surface convection algorithm: outside		DOE-2
Heat balance algorithm		Conduction finite difference
Surface temperature upper limit	C	200
Minimum surface convection heat transfer coefficient	$W/m^2 K$	0.1
Maximum surface convection heat transfer Coefficient	$W/m^2 K$	1000
Difference scheme		Fully implicit first order
Space discretization constant		1000
Relaxation factor		1
Inside surface temperature convergence criteria		0.002
Timesteps per hour		60

solution algorithm was that it does not support the simulation of high conductivity and small thickness materials, such as metal sheets. This limitation was addressed in the simulations of this work by modelling metal materials as mortar materials.

To define the adaptive behaviour of these dynamic technologies, 'Energy Management System' (EMS) was adopted within Energy Plus. In the Appendix, the section "EMS details for each AOF typology" contains the sensors and the algorithms which are needed to define the adaptive behaviour of each facade typology.

Simulated adaptive mechanism with a common simulation strategy

Dynamic technologies need to be combined with static building materials in order to meet the functionalities and requirements of facades beyond the thermal performance (Juaristi et al., 2018a). These combinations, as well as the synergies between different adaptive mechanisms, result in different Adaptive Opaque Façade Typologies, which are presented in section 3, together with their simulation results. Analysed AOF will include, at least, one of the following adaptive heat transfer mechanism, or their combinations:

(a) *Variation of the convective heat transfer of Air Cavities (AC)*: For early-stage design considerations, in the proposed approach simplified values of EN ISO 6946:2007 (2007) were taken to model the resistance that different air cavity configurations would have under different boundary conditions (i.e. differentiating between unventilated, slightly ventilated and ventilated facades), as it is shown in Figure 2.

Air Cavities were modelled in Energy Plus with 'Material:AirGap' class list, as it enables the definition of thermal resistances for construction elements with negligible thermal masses (Table 3).

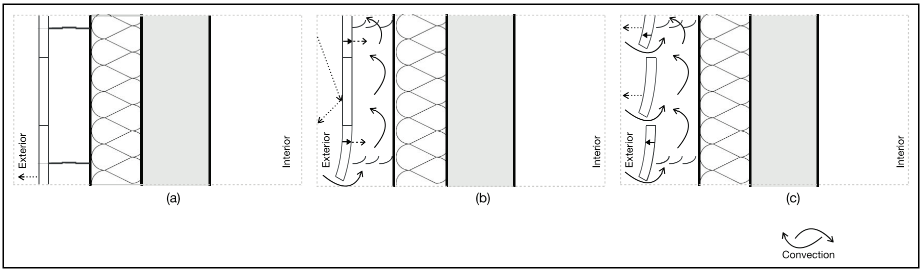

Figure 2. Different Air Cavity configurations: (a) closed joint cladding and closed air cavity, (b) closed joint cladding and open air cavity and (c) open joint cladding and open air cavity.

Table 3. Material:AirGap class list of EnergyPlus to model AC.

Façade component	Configuration	Thermal resistance (m^2 K/W)
Air cavity	Closed Air Cavity (no convective movements)	0.18
Air cavity	Ventilated Air Cavity with closed-joint configuration (convective movements in the air cavity)	0.04
Air cavity	Ventilated Air Cavity with fully open-joint configuration (convective movements in the air cavity with high air velocities)	0.001

(b) *Variation of the solar absorptance of claddings*: as described in the introduction section, advanced and Switchable Coatings can be applied in AOF claddings to achieve a dynamic thermal behaviour on the external facade layer. The key material property which defines this adaptive thermal behaviour is a variable Solar Absorptance (SA) and it can be obtained by integrating automated Kinetic Claddings (KC) or Thermochromic coatings (TCH). The Solar Absorptance of automated Kinetic Cladding is conditioned by (i) the materials of outer and inner claddings and (ii) the geometry of the external cladding (Figure 3).When the Kinetic Cladding is in close-joint configuration, the solar absorptance of the outer cladding layer material (αo) corresponds to the solar absorptance value of the AOF. When the Kinetic Cladding is in open-joint configuration, the material in contact with the insulation layer is the one which captures solar radiation. However, it has shaded areas due to the outer layer. The equivalent solar absorption of the cladding is calculated considering the Opening Degree Coefficient (ODC) of the Kinetic Cladding. When the outer layer of the Kinetic Cladding is parallel to the AOF, the area which receives direct solar radiation (Asa) corresponds to

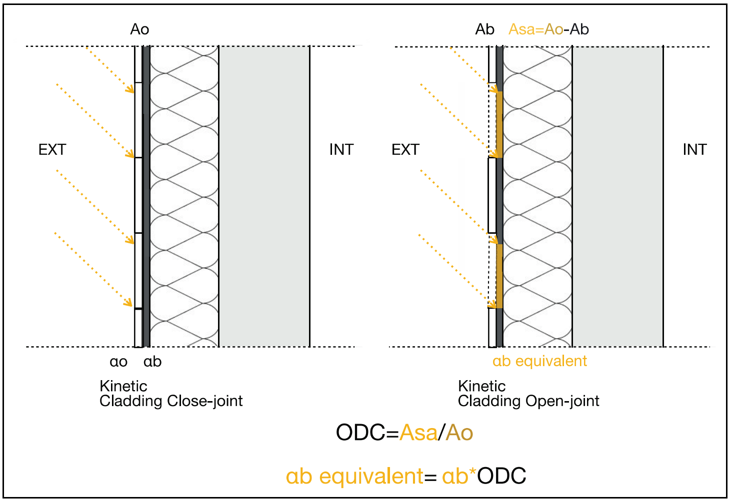

Figure 3. Solar absorptance of the AOF when the Kinetic Cladding is parallel to the AOF.

the opening area of the shading element. Thus, in this paper, it was assumed that when the Kinetic Cladding is in open-joint configuration, the solar absorption of the AOF (αb equivalent) is the product of the solar absorptance of the exposed material (αb) and ODC.

For thermochromic coatings, the solar absorptance depends on their chemical composition. Figure 4 summarizes the solar absorptance variation range of different thermochromic coatings found in literature, which varied their thermal properties when they reached 30°C–31°C surface temperature (Hu and Yu, 2019; Karlessi et al., 2009; Perez et al., 2018; Zheng et al., 2015).

The coatings which have variable solar absorptance were modelled with ‘Material:No mass’ class list by defining one object per each response state. Table 4 summarizes the façade coatings which were modelled at this simulation stage.

(c) *Adaptive insulation components (AIS)*: as it was explained in the introduction, the lack of experimental data forces to make a hypothesis of their adaptation range. The current paper fixes a minimum U-value and therefore a maximum resistance of $4\,W/m^2\,K$ and calculates back the resulting thickness of the AIS to achieve this maximum resistance, so that the minimum resistance can be also defined (as shown in Figure 5).

The variable thermal resistance of Adaptive Insulation components were modelled with ‘Material:AirGap’ class list, as it enables the definition of thermal resistances for construction elements with negligible thermal masses (Table 5).

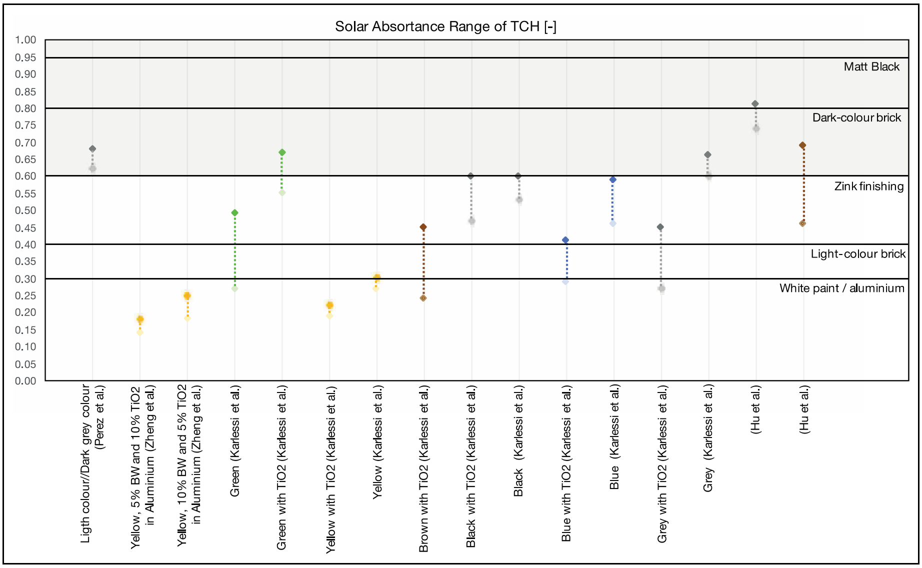

Figure 4. Solar Absorptance Adaptive Range for current technological status (Hu and Yu, 2019; Karlessi et al., 2009; Perez et al., 2018; Zheng et al., 2015).

Table 4. Material:NoMass class list of EnergyPlus to model variable Solar absorptance of claddings. For each technology, the one with the highest adaptation range was selected for the simulation of initial façade configurations.

Material	Thermal resistance (m^2 K/W)	Thermal absorptance (emissivity) [-]	Solar absorptance [-]	Roughness
Green thermochromic coating – Clear colour state (Karlessi et al., 2009)	0.9	0.27	0.27	Medium Smooth
Green thermochromic coating – Dark colour state (Karlessi et al., 2009)	0.9	0.49	0.27	Medium Smooth
Adaptive cladding – Clear colour state*	0.3	0.3	0.3	Medium Smooth
Adaptive cladding – Dark colour state*	0.96	0.9	0.9	Medium Smooth

*The Solar Absorptance of the inner layer of the adaptive cladding (Adaptive cladding – Dark colour state) was estimated based on its opening degree coefficient (ODC = 0.9375%). The Equivalent Solar absorptance of the inner layer is the product of ODC and the Solar Absortance value of the inner cladding material (the Solar Absorptance or a black mortar is equal to 0.96).

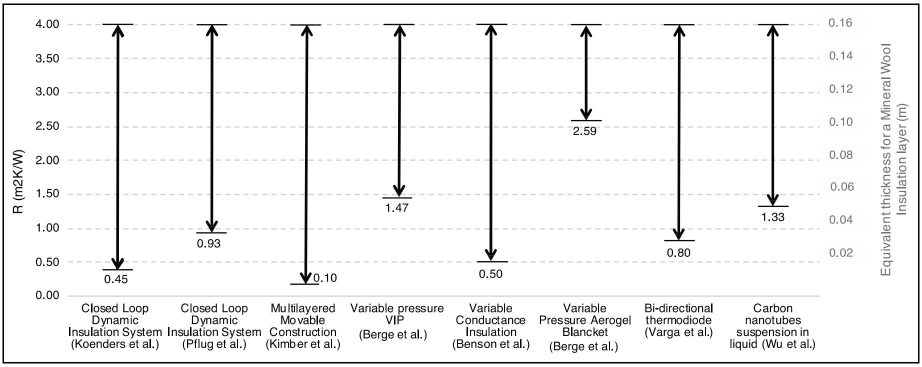

Figure 5. Current technological status of AIS (Berge et al., 2015; Berson et al., 1994; Kimber et al., 2014; Koenders et al., 2018; Pflug et al., 2015; Sunden et al., 2014) and estimation of their adaptation range by fixing the thermal resistance (R) during insulated state equal to 4 m^2 K/W.

Table 5. Material:AirGap class list of EnergyPlus to model AIS. The AIS one with the highest aptation range was selected for the simulation of initial façade configurations.

Façade component	Configuration	Thermal resistance (m^2 K/W)
Adaptive insulation (Kimber et al., 2014)	Insulation in energy conservation state	4
Adaptive insulation (Kimber et al., 2014)	Insulation in conduction state	0.1

The definition of different AOF typologies comes from the combinations of static opaque façade elements with technologies which integrate one or more adaptation mechanisms (i.e. (a) Variation of the convective heat transfer in air cavities, (b) Variation of the Solar Absorptance in claddings and (c) Adaptive Insulation). The technologies considered for the identification of possible AOF typologies with a common simulation strategy were (a) controllable convective heat transfer of air cavities (AC), (b) Thermochromics coatings (TCH) or automated Kinetic Cladding (KC) and (c) Adaptive Insulation components (AIS). These typologies contain either one of the adaptive mechanisms (a, b and c) or a combination of those, together with traditional opaque wall construction elements (i.e off-site walls, heavyweight (Hw) cavity walls and medium/lightweight (Lw) ventilated walls). Besides, the static insulation layer or the AI layer can be placed either in the external, between two static buildings materials or in internal layer according to the features of each Opaque Façade Family. Thus, as Heavy Weight Cavity walls correspond either to (i) traditional façade elements which are refurbished or (ii) to exposed concrete walls, the external placement of the insulation was not analysed for these facades, as their external facade material cannot be changed without altering their aesthetics. The number of integrated adaptation mechanism(s) and the way they are controlled (either passively or actively) define the complexity level of the AOF. In section 3, resulting AOF typologies are presented with their simulation outputs.

Simulation drivers: Meaningful performance indicators

Reduction of thermal energy need is the main driver of this research. This was done considering the following performance metrics:

Annual improvement of the heating energy (IHE) and cooling energy (ICE). These two metrics identify the percentage of the reduction/increase of the Heating and Cooling Energy of the zone, on an annual basis when the performance of AOF is compared to the Static Performance Reference (SPR). They are expressed in % and are calculated according to the following equations:

$$IHE = 1 - \frac{HEAOF}{HESPR}$$

$$ICE = 1 - \frac{CEAOF}{CESPR}$$

where HE is the sensible Heating Energy use demanded per unit area, on an annual basis, by the heating system [kWh/m^2] and CE is the sensible Cooling Energy use per unit area, on an annual basis, by the heating system [kWh/m^2].

Annual total delivered electrical energy (DE). This metric is defined as the total amount of electrical energy that the energy generation system (heat pump) uses, on an annual basis, per unit area, to supply the thermal energy required by the Heating and Cooling systems. It is expressed in kWh/m^2 and is calculated according to the following equation:

$$DE = \left(\frac{HE}{COP} + \frac{CE}{SEER}\right)$$

where COP is the average Coefficient of Performance of the heat pump system during winter period and the SEER is the Seasonal Energy Efficiency Ratio of the heat pump in the cooling period.

Annual improvement of total delivered energy (IDE). This metric refers to the percentage of the reduction/increase of the Delivered Energy, on an annual basis, when the output of AOF and SPR are compared. It is expressed in % and is calculated according to the following equation:

$$IDE = 1 - \frac{DE\ AOF}{DE\ SPR}$$

Annual adaptation cycle. This metric quantifies the number of times the AOF changes its configuration or characteristics. To get this information from the simulations, the model has as an output the 'Construction Index'. The Annual Adaptation Cycle is calculated by counting how many times this index changes.

Performance benchmark

Static Performance Reference (SPR) works as comparison benchmarks to calculate the potential improvements in HE, CE and DE when AOF are applied. To identify which is a good performing SPR in each location, the thermal performance of eight possible static opaque facades were compared (Appendix Table A1). These static opaque facades were defined based on different construction options (Figure 6) and by modifying the building materials which affect the Solar Absorptance of the cladding and the Admittance of the building envelope. The thickness of the insulation layer was calculated for each city according to the *U*-value recommended/required by the national regulations (Appendix Table A2), Among the eight possible static opaque facades, the one with less DE served to detect the SPR of each location and established the HE, CE and DE benchmark aims to improve by the design of AOF (Appendix Table A3). For the case study climates of the current paper, SPR is always a heavyweight façade which is built with concrete walls and it has an intermediate layer of mineral wool. The exterior finishing has a low solar absorptance, as it is painted in white. The selected climates have mild-winter seasons and warm summers, even if the HE and CE vary. This could explain why the aforementioned SPR is always the most preferable one among the analysed static opaque façades.

Define test case building models

The simulation model consisted on a reference room representing a typical living room of a residential building, surrounded by similarly conditioned spaces/

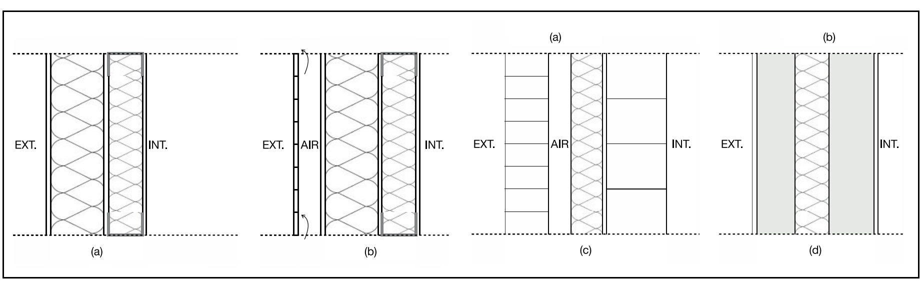

Figure 6. Representative static opaque facade typologies: (a) Lightweight off-site wall, (b) Lightweight/medium-weight ventilated wall, (c) Medium-weight/heavyweight cavity wall, and (d) Heavyweight exposed concrete wall with a white painting finishing: this is the Static Performance Reference for the analysed case studies.

Table 6. Usability and energy parameters which were used to define the Simulation model.

Parameter type	Units	Parameter value (for fraction = 1)
People	m^2/person	28.3
Lights	W/m^2	9.6
Electric equipment	W/m^2	3
Ventilation (Flow rate per person)	m^3/s-person	0.007
Infiltration rate	1/h	0.5

apartments, within a multi-story residential building (such that all the walls not exposed to the outdoor environment can be considered adiabatic). The room size is 4.5 m wide × 4 m deep × 2.5 m high. Only west façade is exposed to external boundary conditions. It is partially glazed (Window-to-wall ratio WWR = 19%) with a Double-Glazing Unit (DGU), which has Low-E glazing on the internal side and with a 16 mm air cavity. Besides, it has a controlled shadow system on the outside side of the window (see the details in the Appendix, Tables A5–A7).

Schedules relative to occupation, ventilation and equipment were adopted from (UNE-EN 16798-1, 2020) and the power density for lighting from (ANSI/ASHRAE/IES Standard 90.1-2010, 2010). Tables 6 and 7 summarize the usability and energy parameters which served to set the simulation model. The HVAC system was defined as ideal systems, that is able to maintain the set-point (20°C for heating and 26°C for cooling) and setback temperatures (16°C for heating). The set-point temperatures were assumed to be maintained at any moment of the year, according to the external boundary conditions and the occupation rate. The overall coefficients of performance were calculated considering that the energy was calculated employing a heat pump and therefore, the COP of the heating system was defined as 2.5, whereas the cooling system SEER was set equal to 3.5.

Simulation results: Consideration of additional remarkable outputs beyond energy use reduction

Simulations serve to assess if AOF options have a better thermal performance than Static Performance Reference (the characteristics of simulated AOF are are detailed in the Appendix: Table A8, A9 and A10). The analysis of IHE, ICE and IDE reports if this target is achieved and the results of the absolute reduction obtained for HE, CE and DE values illustrate if the obtained benefit can have a sufficient impact on the annual thermal energy use (Appendix, Table A11, A12).

Besides, simulation outputs can also give interesting remarks about the total number of adaptation cycles over the simulation period. This output is interesting (i) to better understand how the proposed AOF works, as it gives an approximate idea about the distribution of adaptation cycles over a year and a day; and (ii) to calculate the total number of cycles that the product developer must guarantee for

Table 7. Building operation parameters.

All days	00–06	06–07	07–09	09–11	11–13	13–15	15–16	16–17	17–19	19–22	22–24
Occupancy (fraction)	1	0.5	0.5	0.1	0.1	0.2	0.2	0.5	0.5	0.8	1
Equipment (fraction)	0.5	0.5	0.7	0.5	0.6	0.6	0.5	0.5	0.7	0.8	0.6
Heating set point (°C)	16	20	20	20	20	20	20	20	20	20	16
Cooling set point (°C)	26	26	26	26	26	26	26	26	26	26	26
All days	00–05	05–06	06–10	10–18		18–19	19–20	20–21	21–22	22–23	23–24
Lighting (fraction)	0.1	0.3	0.45	0.3		0.6	0.8	0.9	0.8	0.6	0.3

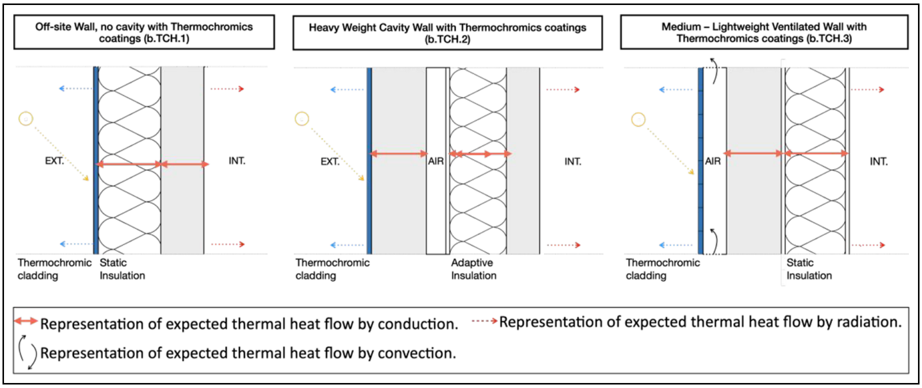

Figure 7. AOF typologies with Level 1 of complexity.

the total life-cycle of the building material/component. This information, together with the complexity level of different AOF design options reveals if the additional sophistication that implies the integration of the selected dynamic technologies.

Results

Simulation results for AOF typologies with Level 1 of complexity

The following section shows the simulation results for the AOF typologies which have a single dynamic technology which is passively controlled. Their adaptation strategy is the variation of the Solar Absorptance of claddings through thermochromic coatings. By applying these coatings in opaque facades, the solar absorptance of the external cladding decreases when it reaches 30°C–31°C. These coatings were simulated for three possible opaque façade typologies (Figure 7).

According to the simulation results, most of the times these façade typologies do not offer an Annual Improvement of total Delivered Energy (Figure 8). Athens is the only location where thermochromic coatings might have a positive impact if they are integrated in Off-site heavyweight walls and Mediumweight (Mw) Ventilated walls. The reason why no or little improvement is achieved is due to the fact that the static benchmark performs better under cooling periods, as its solar absorptance is lower. The thermochromic coating does not either reduce substantially the heating demand, as its solar absorptance decreases when it reaches 30°C even during heating periods, where having higher temperatures on the outer cladding is beneficial (detailed results of IHE and ICE are available in the Appendix, Table A12).

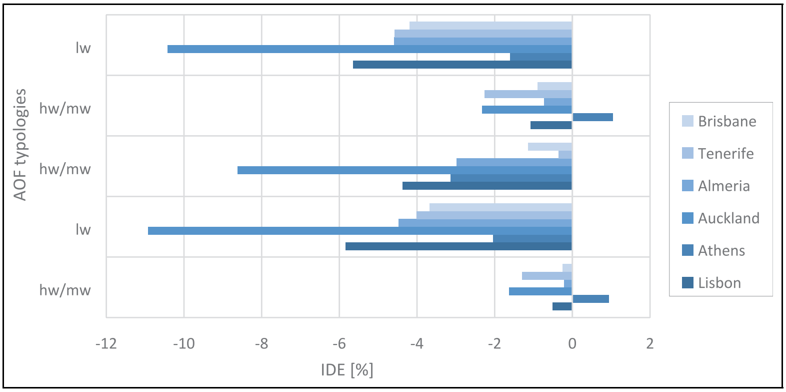

Figure 8. Simulation results for AOF typologies with Level 1 of complexity.

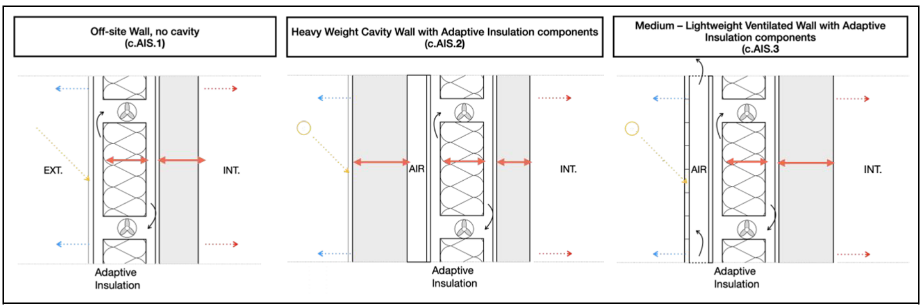

Figure 9. AOF typologies integrating Adaptive Insulation components and with Level 2 of complexity.

Simulation results for AOF typologies with Level 2 of complexity

AOF with Level 2 of complexity integrates one actively controlled dynamic technology (applied control strategies are available as Supplemental Material):

(a) *Variation of the convective heat transfer of air cavities*: Figure 2 represents the adaptation mechanism of controllable air cavities. The aim is to enhanced/diminished heat loses of the wall for each boundary condition by implementing the most suitable air-cavity configuration. Its integration in opaque facades results in a Lightweight/Mediumweight Ventilated Wall with controllable convective heat transfer of air cavities (a.AC.3).

(b) *Variation of the solar absorptance of claddings*: Figure 3 represents the adaptation mechanism of an Off-site Wall, with no cavity with automated Kinetic Cladding (b.KC.1). The geometry changes of the outer layer, which varies the solar absorptance of the opaque facade, is actively controlled.

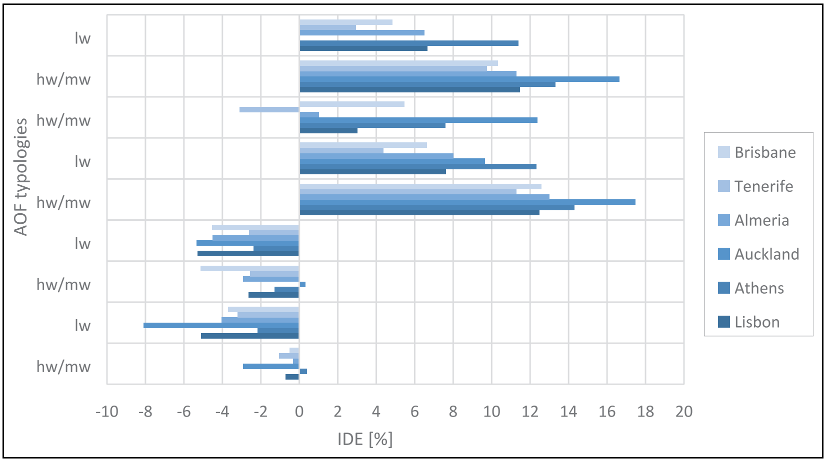

Figure 10. Simulation results for AOF typologies with Level 2 of complexity.

(c) *Adaptive insulation*: closed AI components can be integrated in any type of opaque facades, as illustrated Figure 9, to control the heat transfer through the wall.

The results of Figure 10 evidence that Lightweight Ventilated Wall with controllable convective heat transfer of air cavities (a.AC.3) and Off-site Wall, with no cavity with automated Kinetic Cladding (b.KC.1) perform worse than the Static Performance Benchmark facade. As explained in section 2.5, Heavyweight Exposed concrete Wall with low solar absorptance is the best performing static opaque façade typology. The aforementioned AOF typologies do not have as much thermal mass as the Static Performance Benchmark. According to the obtained results, it seems that having high thermal mass is a more effective design strategy than the controlling of the air cavity configuration or the adapting the solar absorptance of the exterior finishing with a Kinetic Cladding.

On the contrary, the simulation outputs indicate substantial reductions in thermal energy use when Adaptive Insulation Components are integrated. For analysed six climates, the Offsite Wall with no cavity and with one Adaptive Insulation Component (c.AIS.1) is the best performing AOF typology, especially when the interior layer has high thermal mass. The Annual Improvement of total Delivered Energy goes from 11.30% in Tenerife to 17.47% in Auckland. Mediumweight Ventilated Wall (c.AIS.3) perform slightly worse than c.AIS.1. The additional thermal resistance due to the ventilated air cavity makes the adaptation range of the thermal heat transfer mechanism slightly lower than for c.AIS.3, which would explain the reduction in the obtained IDE. Similarly, the thermal energy reduction is even less effective for Heavyweight cavity wall with Adaptive Insulation components (c.AIS.2), as the thermal resistance of the closed-cavity is higher. Besides, in

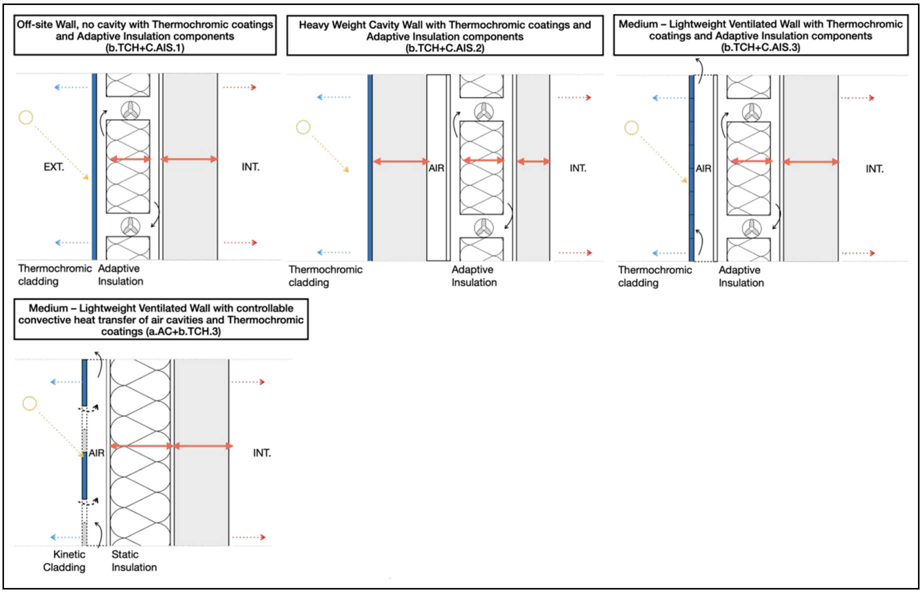

Figure 11. AOF typologies integrating Adaptive Insulation components and with Level 3 of complexity.

Tenerife, c.AIS.2 perform worse than the Reference Static Benchmark, most probably due to its higher overall thermal resistance.

Simulation results for AOF typologies with Level 3 of complexity

AOF with Level 3 of complexity combine two adaptation mechanism, one of which is passively controlled and another one which is actively control. The passively controlled adaptation mechanism is the Variation of the Solar Absorptance of claddings which can be achieved by integrating thermochromic coatings in the external layer. The actively controlled adaptation mechanisms can be (a) the variation of the convective heat transfer of air cavities or (c) the Adaptive Insulation. Figure 11 summarizes the possible AOF typologies with Level 3 of complexity.

Figure 12 shows the simulation results for these AOF typologies. When thermochromic coatings are applied in Heavy Weight Cavity Walls or Ventilated walls which also integrate Adaptive Insulation components, the IDE improves less than 2% with respect to the similar typologies with traditional coating materials (c.AIS.2 and c.AIS.3). The Energy Use for the Off-site Wall, no cavity with Thermochromics coatings and Adaptive Insulation components (b.TCH + c.AIS.1) is higher than for the Reference Static Benchmark, except from Auckland and even in this case, the thermochromic has not a positive impact, as its static cladding version (c.AIS.1) has a higher IDE.

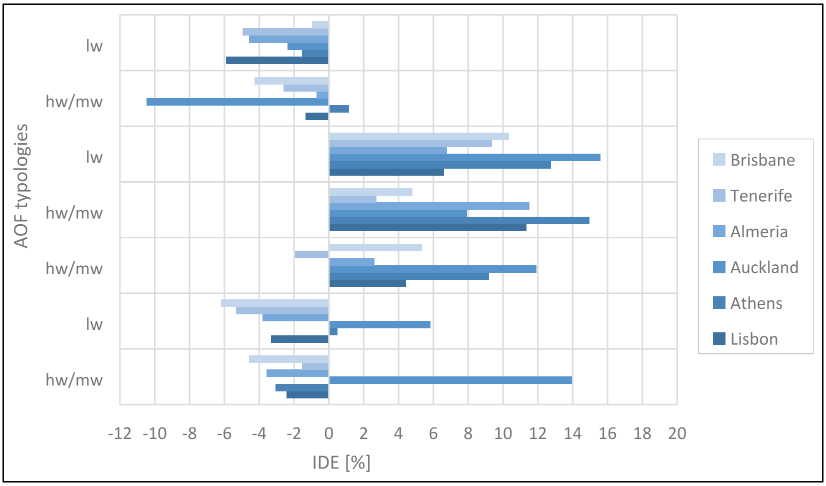

Figure 12. Simulation results for AOF typologies with Level 3 of complexity.

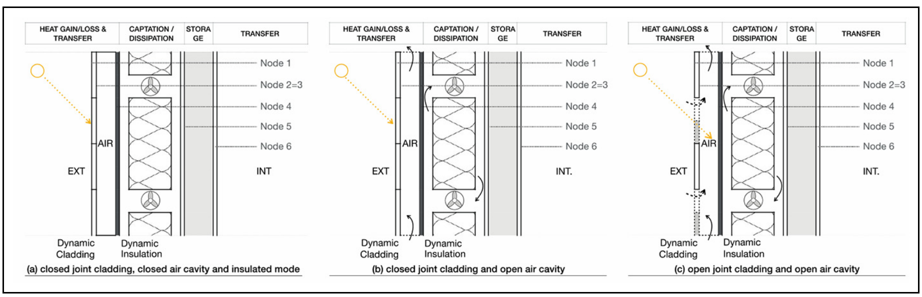

Figure 13. AOF typologies integrating Adaptive Insulation components and with Level 4 of complexity.

Simulation results for AOF typologies with Level 4 of complexity

The most complex AOF typologies integrate multiple dynamic technologies which are actively controlled (Figure 13). Off-site Wall, no cavity with automated Kinetic Cladding and Adaptive Insulation components (b.KC + c.AIS.1) are able to manage both the solar absorption and the heat transfer through the wall, therefore this façade can dissipate thermal energy when indoor spaces are overheated and can also contribute to reduce heating demand by obtaining heat gains from the outdoor medium when the incident solar radiation warms up the exterior cladding. Ventilated Wall with controllable convective heat transfer of air cavities and with

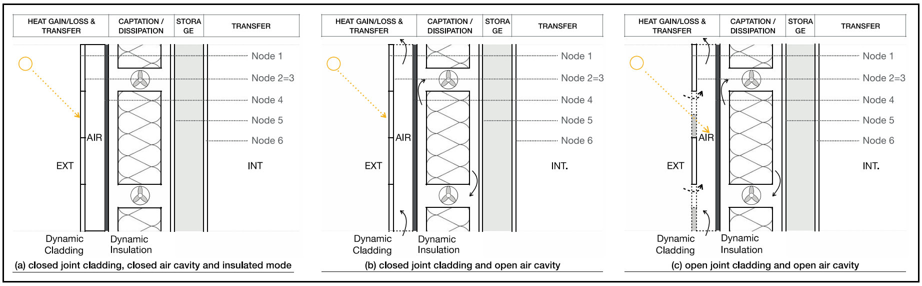

Figure 14. Possible façade configurations and distribution of nodes for a.AC + b.KC + c.AIS.3 façade typology.

automated Kinetic Cladding (a.AC + b.KC.3) can autonomously control the heat gains and loss through radiation and convection.

Ventilated Wall with controllable convective heat transfer of air cavities, with automated Kinetic Cladding and Adaptive Insulation components (a.AC + b.KC + c.AIS.3) has a more complex behaviour (Figure 14).A detailed analysis of simulation results enables a better understanding.

The variations in the façade configurations were modelled in Energy Plus with different construction index, as exposed in section 2.3. This simulation strategy enables getting as outputs the distribution of the node temperatures, which are also the temperatures of each façade layer. During heating demand period, this façade has two possible configurations:

- 'KC Low SA, ACa, AIS insulated mode': the envelope configuration contributes to reduce the energy loses between indoor and outdoor environment. The external cladding is in close-joint configuration and the air cavity is in non-ventilated mode to avoid thermal loses by convection. AIS is behaving in its insulated mode. The Solar Absorptance of the façade is low, as the external cladding finishing material is aluminium.
- 'KC High SA, ACc, AIS conduction mode': solar heat gains want to be captured, by opening as much as possible the joints of the Kinetic Cladding, exposing the internal cladding material (which has higher solar absorptance material), eliminating the thermal buffer effect of the air cavity and by activating the conduction mode of the AIS.

The adaptation from the protection state to the conduction state happens when the temperature of the outside surface is higher than the interior surface temperature of the AIS (Node 5). It changes again to the protection state once that the interior surface temperature of the AIS is lower than the outside surface temperature of the AIS (Node 4). Figure 15 illustrates how the temperature of each node varies (left Y axis) according to the construction index (right Y axis) and boundary conditions.

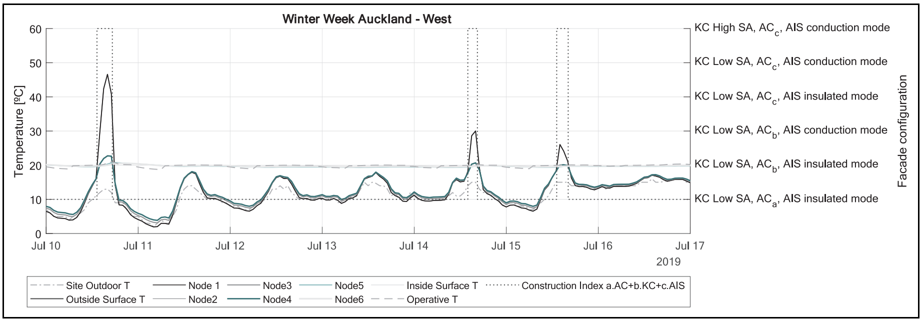

Figure 15. Adaptive behaviour of a.AC + b.KC + c.AIS.3 façade typology during a winter week in Auckland.

This figure represents the performance of the AOF oriented to the West, during a winter week in Auckland. In three afternoons (10, 14–15 July) the façade captures the solar heat gains of the outer layer of the envelope to reduce the Heating Energy. During the remaining time the envelope configuration contributes to reduce the energy loses between indoor and outdoor environment.

During cooling demand period, the dissipation of internal heat gains can be achieved by varying AIS behaviour (i.e. from insulated mode to conduction mode) and by promoting convective heat losses in the air cavity (ACb). When wind velocity is high, the resistance of the air cavity reduces even more (ACc). Besides, when there is cooling demand and the temperature in the external surface of the AIS is lower than in the interior surface of the AIS, the AIS adapts to the conduction mode. Figure 16 shows a summer week in Auckland and illustrates how for a west oriented façade, Ventilated Wall with controllable convective heat transfer of air cavities, with automated Kinetic Cladding and Adaptive Insulation components effectively reduces Cooling Energy need by dissipating the internal heat gains in the morning and afternoon.

Figure 17 summarizes the results for the three AOF typologies with complexity Level 4. What stands out from this table is that Off-site Wall, no cavity with automated Kinetic Cladding and Adaptive Insulation components (b.KC + c.AIS.1) and Medium–Lightweight Ventilated Wall with controllable convective heat transfer of air cavities, with automated Kinetic Cladding and Adaptive Insulation components (a.AC + b.KC + c.AIS.3) are the façade typologies reducing the most the Annual total Delivered Energy (DE) compared to the energy performance of SPR for all the analysed climates. Thus, the variation of the Solar Absorptance of the cladding and the modification of the intensity of the heat transfer by means of Adaptive Insulation (AIS) seems to have a positive impact on the thermal performance. Among the studied locations, Auckland seems to be the one with better results when these AOF are applied. Its IDE is equal to 34% for the façade typology with no air cavity and its IDE is about 30% when the AOF has also an

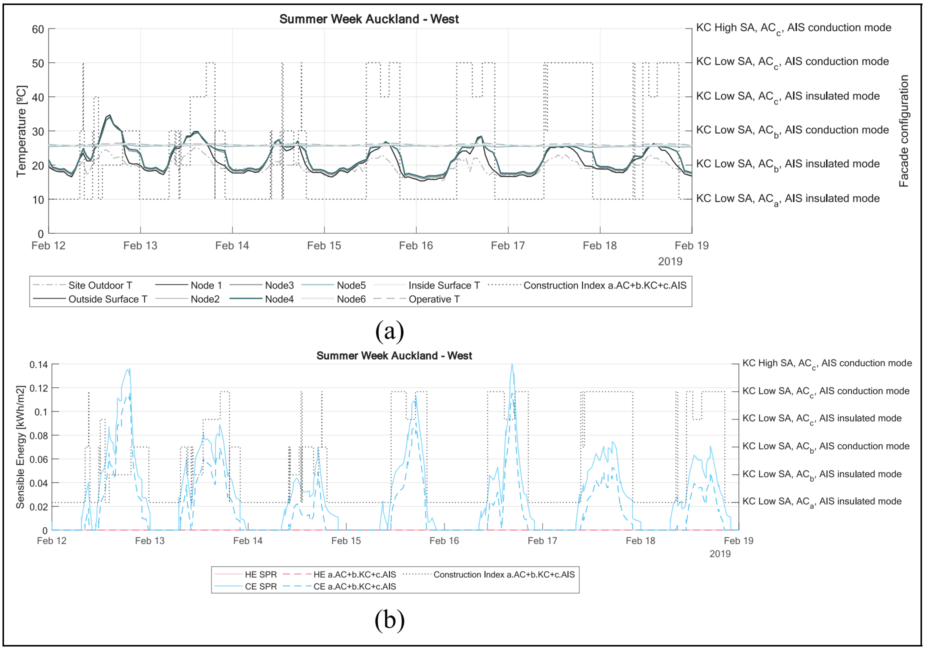

Figure 16. Adaptive behaviour of a.AC + b.KC + c.AIS façade typology during a summer week in Auckland. Simulation outputs: (a) temperature in each node and facade configuration (construction index) for each simulation time-step, and (b) Heating Energy and Cooling Energy and facade configuration.

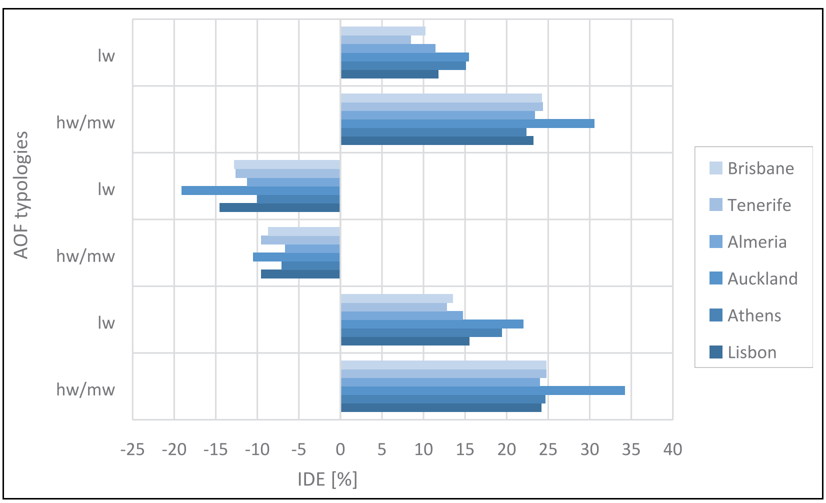

Figure 17. Simulation results for AOF typologies with Level 4 of complexity.

advanced ventilated air cavity. Auckland is also the climate which has the lowest DE and this could have influenced its higher improvement.

In the same vein, the application of ventilated air cavities does not exclude the improvement of the overall thermal performance. Yet they do not have a better impact than AOF typologies with no ventilated air cavities. Besides, no increase in DE is detected with respect to SPR when the variation of the convective heat transfer of air cavities is the only integrated adaptive thermal behaviour, or when they are combined with Kinetic Claddings (i.e. a.AC.3 and a.AC + b.KC.3). Overall, lightweight façade configurations offer less improvement with respect to the SPR than heavyweight façade configurations

Impact of the design decisions on the thermal performance, complexity level and adaptation cycles

The evaluation of the most promising AOF is enlarged and additional simulation outputs are analysed to understand more in detail the opportunities and challenges of these facades. As exposed in the previous section, the most promising AOF typologies are:

-c. AIS.1: Off-site wall with no air cavity which integrates an Adaptive Insulation component and its external cladding has low solar absorptance
-b. KC. + c.AIS.1: Off-site wall with no air cavity which has an actively controlled Kinetic Cladding, which is able to vary the Solar Absorptance of the façade and which integrates an Adaptive Insulationcomponent.
-a. AC + b.KC + c.AIS.3: Mediumweight Ventilated Wall which has an actively controlled Kinetic Cladding, which is able to vary the Solar Absorptance of the façade and the convective heat movements of the air cavity and which integrates an Adaptive Insulation component.

Adaptation range of Kinetic Claddings depends both on the selected finishing façade materials and on the opening degree of the exterior cladding. Initial round of simulations assumed the geometry which can offer the highest adaptation range (60%). The parameter analysis serves to quantify the impact on the thermal performance when the exterior claddings have an adaptation range of 6% and 28%.

Figure 18 presents how the variations in the outer cladding geometry have a little impact on the IDE. Auckland is the place where the reduction of the adaptation range minimizes more the IDE, and even though, the difference between the two design options is inferior to 2%. for Medium – Lightweight Ventilated Wall with controllable convective heat transfer of air cavities, with automated Kinetic Cladding and Adaptive Insulation components (a.AC + b.KC + c.AIS.3) When looking at HE, the application of geometry with a smaller opening degree coefficient has a more significant negative impact. For instance, IHE Almeria IDE is reduced to 80% for the design geometry providing 28% of adaptation range and

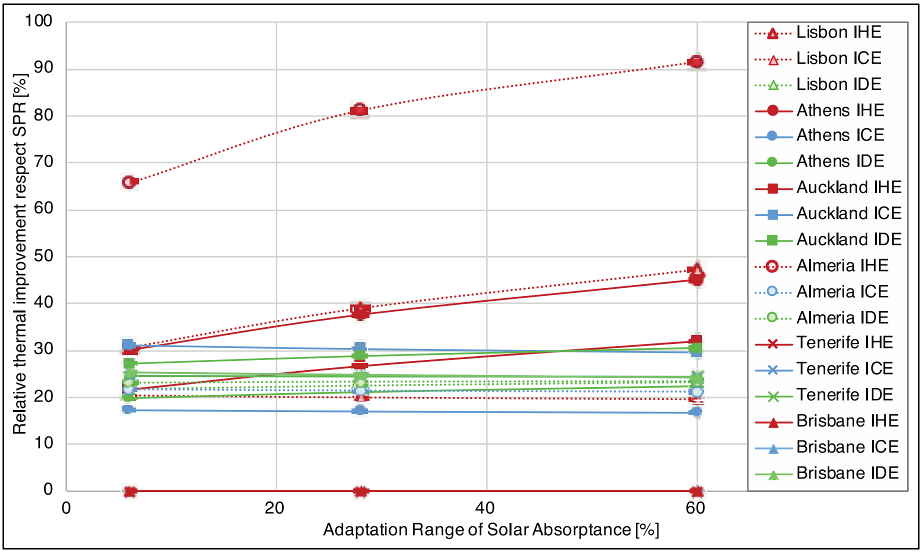

Figure 18. Sensitivity analysis for IDE [%] results in relation to the solar adaptation range variation.

around 65% for the cladding with 6% of adaptation range. Even though, its IDE hardly varies, as the HE of Almeria is very low for both the analysed façade typology, ICE is almost not affected by geometry changes. This outcome is not surprising, as the outer layer of the simulated facade options have low solar absorptances. Thus, for the analysed case studies, the presented designs of the outer layer geometries can be considered as candidate design-options because the IDE of examined locations are barely cut down.

The complexity of the AOF options should be considered to evaluate the potential of an adaptive façade respect the static benchmark facade. The Off-site Wall, no cavity with Adaptive Insulation components (c.AIS.1) is extrinsically controlled by a single dynamic technology. On the other hand, the Off-site Wall, no cavity with automated Kinetic Cladding and Adaptive Insulation components (b.KC + c.AIS.3) and the Medium–Lightweight Ventilated Wall with controllable convective heat transfer of air cavities, with automated Kinetic Cladding and Adaptive Insulation components (a.AC + b.KC + c.AIS.3) need the integration of multiple dynamic technologies which are actively controlled. Moreover, the most complex façade configuration also results in more annual adaptation cycles than simpler solutions (Figure 19) For the examined case studies, the Medium–Lightweight Ventilated Wall with controllable convective heat transfer of air cavities, with automated Kinetic Cladding and Adaptive Insulation components (a.AC + b.KC + c.AIS.3) can have more than 2500 adaptation cycles per year. This means that the kinetic cladding, the moving elements which control the configuration of the air cavity and AIS needs to guarantee around 4 daily changes

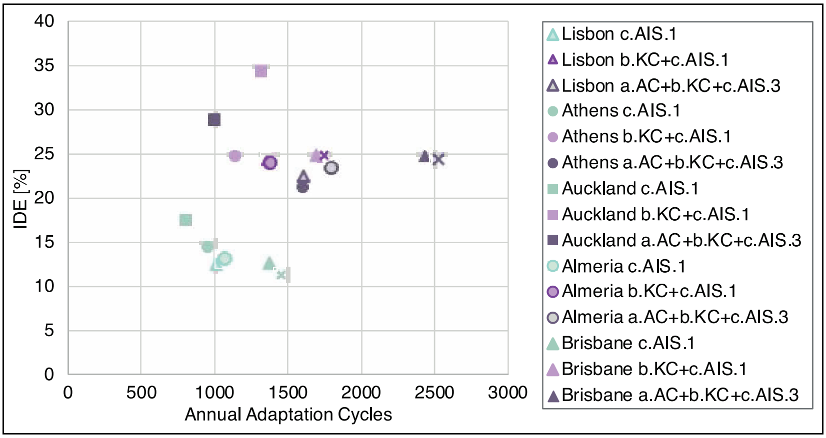

Figure 19. Annual Adaptation Cycles for final design options in different locations and achieved IDE. Both the design and the climates will have an effect on the life-cycle that the AOF must guarantee.

(Figure 19). The Adaptive Insulation component of the Off-site Wall, no cavity with automated Kinetic Cladding and Adaptive Insulation components (c.AIS.1) has less than 1500 adaptation cycles per year, which would be less than 2 daily changes. These results depend on the façade configuration, control definition and external boundary conditions. Thus, designers need to consider that the adaptation cycles of dynamic technologies will also depend on the climates where they are located.

All in all, the Off-site Wall, no cavity with automated Kinetic Cladding and Adaptive Insulation components (b.KC + c.AIS.3) and the Medium–Lightweight Ventilated Wall with controllable convective heat transfer of air cavities, with automated Kinetic Cladding and Adaptive Insulation components (a.AC + b.KC + c.AIS.3) imply a higher sophistication and complexity, but their ability to adapt more times also lead to higher IDE in the analysed case studies (Figure 19).

Figure 20 summarizes the output of the three candidates AOF design options and illustrates the reduction in DE, HE and CE [kWh/m^2] of final design options with respect to the Static Performance Benchmark. It shows how solutions with automated Kinetic Cladding (KC) and Adaptive Insulation Component (b.KC. + c.AIS.1), which KC has an adaptation range of 60%, is the best AOF in all locations, as it is the one reducing the most HE value. The results also demonstrate that the increasing the complexity level enhances the thermal performance.

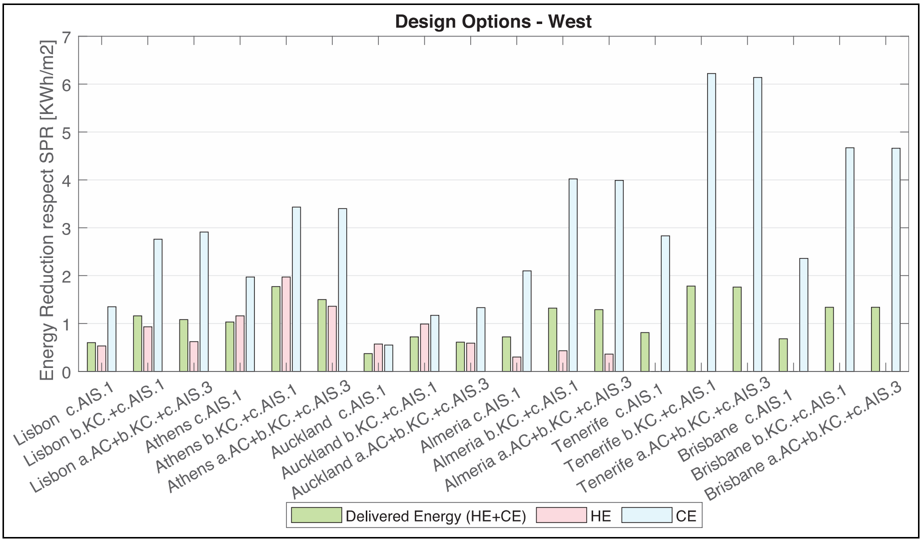

Figure 20. DE, HE and CE reduction of final design options with respect to DE, HE and CE of the SPR in different locations.

Discussion

The presented study supports evidence from previous simulations works (Jin et al., 2017; Park et al., 2015; Pflug et al., 2017) in the positive impact of heavyweight Adaptive Opaque Façade configurations for reducing Delivered Energy. In accordance with previous studies, presented annual results in absolute values [kWh/m^2] have demonstrated that Adaptive Insulation effectively reduces Cooling Energy of the room, and in a less significant way, Heating Energy. When the Heating Energy reduction was calculated regarding SPR in absolute values, the absolute reduction was not very high, as the analysed climates have low Heating Degree Days (HDD). Even though, the little heating energy needs which Static Performance Reference had almost disappeared if AOF were properly applied. This outcome suggests that the application of complex AOF typologies in residential buildings, which are able to capture solar heat gains and dissipate internal heat gains when necessary (such as analysed c.AIS + b.KC.1 and a.AC + b.KC + c.AIS.3 façade configurations), could nearly eliminate the need of heating systems (e.g. Almeria, Auckland and Lisbon). Thus, analyzing the results in relation to Static Performance Reference [%], an Annual Improvement of the Cooling Energy (ICE) of the room about 20%–25% was achieved for best AOF configurations and the Annual Improvement of the Heating Energy was always superior to the 45%.

All the results in literature are in the same direction and their differences are mainly due to the different adaptation ranges, the selected control strategies or climates and building patterns of use. The current work modelled the behaviour of

Adaptive Insulation by assuming an adaptation range of 4–0.10 m^2 K/W. The results reported by (Park et al., 2015; Pflug et al., 2017) showed a less significant Annual Improvement of the Heating Energy of 10% and a more significant improvement of the Cooling Energy of 40%–55%. This difference in results could be partially due to the fact that in the previous research, the AIS was modelled to have a thermal resistance of 2 and 2.8 m^2 K/W respectively. Thus, they perform worse under Heating Demand conditions and better under Cooling Demand situations. Besides, the good results of the presented study regarding IHE correspond to those façade typologies which do not only integrate an AIS system, but they also have a kinetic cladding which actively modulates solar heat gains on the façade surface. The present work modelled for the first-time synergies between different adaptive mechanisms in a same AOF system. The identified novel AOF typologies were proven to be more complex, but also more efficient from the thermal performance point of view. Moreover, the integration of complex adaptation mechanisms offers such benefits when they are in highweight/mediumweight façade configurations, which means that effectively charging and discharging the thermal mass of AOF has a crucial effect. This outcome is also in line with the results reported by Jin et al. (2017).

The reason why in this paper the Cooling Energy was not reduced as many as in other works could be in part due to the control strategy definition. When there was no cooling demand, the adaptive insulation was in insulation state and this could have caused overheating periods. A further optimization of the control-strategy would most probably enhance the obtained results. In fact, this is consistent with literature, as Jin et al. (2017) noted that advanced control strategy enhanced considerably the thermal performance. They reported an Annual Improvement of the Heating Energy of 60% and of Cooling Energy of up to 69% with the use of Model Predictive Control, for an optimized adaptive insulation wall system (adaptive insulation with comparable range of variation to this study, external to the thermal mass of the wall).

The application of ventilated air cavities which can control convective heat transfer did not enhance the thermal performance significantly. Current research used a rule-based control within EnergyPlus by using Energy Management System to model this adaptive mechanism. The defined control measured the wind velocity of the outside conditions and assessed if the façade was under heating or cooling demand conditions to set the best performing façade configuration. However, the convective movements altering the thermal resistance of the ventilated air-cavity are also affected by incident solar radiation, the material of the façade cladding and its geometry (Ibañez-Puy et al., 2017; Sánchez et al., 2017). Future works should indicate in a more detailed way how different boundary conditions affect the thermal resistance of air cavities.

According to the results of the present work thermochromic coatings do not reduce the annual total Delivered Energy. By reviewing the literature, only one study evaluated the Thermochromics integration in opaque facades and the thermal energy reduction at building level (Zheng et al., 2015). They reported that thermochromic coatings perform more favourably than cool coatings. Nevertheless, they also stated that the effect of these thermochromic coatings were more notable in the places where the temperatures varies greatly between seasons. This would explain why the effect of thermochromic coatings is not visible in the analysed case study climates, as they have mild-winter seasons and warm summers. However, this explanation does not seem applicable to variable solar absorptance when it is actively controlled, as the current paper demonstrates that they can have a positive impact on the Annual Improvement of total Delivered Energy. However, Thermochromic claddings analysed in this study could have had a poorer thermal performance not only due to the fact that they were passively controlled, but also because their adaptation range was limited to the 20%, whereas the studied Kinetic claddings which high potential had an adaptation range of 28%–60%. Thus, more research is needed to understand the possible Thermochromics contribution to reduce thermal energy demand.

Conclusion

The presented research shows the simulation results of 15 AOF typologies within Energy Plus, by using its conduction finite difference (CondFD) solution algorithm and Energy Management system. The simulation strategy was demonstrated to be compatible with different characteristics of AOF typologies and adaptive thermal mechanisms. For the first time, AOF typologies able to vary the solar absorptance of Kinetic Claddings and AOF which integrate controllable convective heat transfer of air cavities were simulated. As far as the authors know, this was also the first study analysing the thermal performance of AOF typologies integrating synergies between different adaptive mechanisms. The presented simulation based assessment also enables for the first time a more comprehensive performance evaluation by considering other operational aspects, such as the annual number of adaptation cycles or the nature of the adaptive mechanisms, which defines the operational complexity needed to integrate the proposed dynamic technologies.

Regarding the effect of different AOF typologies and façade configurations, the present study has shown for the analysed climates (which have mild-winter seasons and warm summers) and for residential building that:

- Between the different adaptive strategies, the variation of the heat transfer by means of Adaptive Insulation components has the most significant impact on the thermal energy use reduction. The variation of the solar absorptance has also a significant positive impact, especially in IHE, but only if this variation is actively controlled and if is in combination with Adaptive Insulation components. AOF typologies which do not integrate Adaptive Insulation components do not provide any improvement with respect to the static reference benchmark;
- The annual adaptation cycles of specific dynamic technologies depend on the specific climate, therefore it is crucial to quantify and potentially limit them in order to reduce the complexity of the control while improving service life;

- The integration of more complex adaptive mechanism combinations and active technologies derive into a higher number of adaptation cycles, but for most analysed climates it also resulted into doubling the overall energy performance. Therefore, the balance between the complexity of the designed AOF system and the obtained benefits need a careful consideration on a case by case basis.

A natural progression of this work is to include transparent and translucent Adaptive Facades and advanced ventilation strategies into the simulation method, in order to reduce even more the thermal energy demand. This would assist designers to propose ambitious and sophisticated building envelopes for Nearly Zero Energy Building (NZEB). Besides, further studies in advance control strategies for Adaptive Opaque Facades, such as Artificial Intelligence algorithms and Model Predictive Controls, might enlarge the obtained benefits. Last but not least, more experimental assessments are needed to enhance the simulation models of the adaptive thermal mechanisms.

Acknowledgements

The authors would like to thank COST Action TU1403 'Adaptive Façade Network' for providing excellent research networking. The corresponding author would also like to gratefully acknowledge the Government of Navarra for the grant 'Ayudas Predoctorales de Movilidad Internacional'.

Declaration of conflicting interests

The author(s) declared no potential conflicts of interest with respect to the research, authorship, and/or publication of this article.

Funding

The author(s) disclosed receipt of the following financial support for the research, authorship, and/or publication of this article: This paper is part of the PhD research project titled "Adaptive Opaque Facades: a Performance Based design Method", promoted by *Asociación de Amigos de la Universidad de Navarra and Banco Santander*.

ORCID iDs

Miren Juaristi https://orcid.org/0000-0001-8760-1746
Tomás Gómez-Acebo https://orcid.org/0000-0001-6559-1313

Supplemental material

Supplemental material for this article is available online.

References

Aelenei L, Aelenei D, Romano R, et al. (2018) *Case studies – Adaptive facade network* (L Aelenei, D Aelenei, R Romano, et al. eds). TU Delft open for the COST Action 1403 adaptive facade network editors. Available at: http://tu1403.eu/wp-content/uploads/Vol-3-1_for-web-Open-Access-9789463661102.pdf (accessed 5 August 2021).

ANSI/ASHRAE/IES Standard 90.1-2010 (2010) Energy standard for buildings except low-rise residential buildings. American Society of Heating, Refrigerating and Air-Conditioning Engineers.

Arıcı M, Bilgin F, Nižetić S, et al. (2020) PCM integrated to external building walls: An optimization study on maximum activation of latent heat. *Applied Thermal Engineering* 165: 1–13.

Aschehoug Andresen I, Heiselberg P, et al. (2008) *Annex 44. Integrating Environmentally Responsive Elements in Buildings*. Aalborg, Denmark. Available at: https://iea-ebc.org/projects/project?AnnexID = 44 (accessed 5 August 2021).

Attia S, Bilir S, Safy T, et al. (2018) Current trends and future challenges in the performance assessment of adaptive façade systems. *Energy and Buildings* 179: 165–182.

Baker PH (2003) The thermal performance of a prototype dynamically insulated wall. *Building Services Engineering Research and Technology* 24(1): 25–34.

Berge A, Hagentoft CE, Wahlgren P, et al. (2015) Effect from a variable U-value in adaptive building components with controlled internal air pressure. *Energy Procedia* 78: 376–381.

Berson D, Potter T and Tracy C (1994) Design of a variable conductance vacuum insulation. In: *SAE 1994 annual meeting*, Detroit, MI. SAE International.

Bianco L, Cascone Y, Avesani S, et al. (2018) Towards new metrics for the characterisation of the dynamic performance of adaptive façade systems. *Journal of Facade Design and Engineering* 6(3): 175–196.

Cabeza LF, Castell A, Barreneche C, et al. (2011) Materials used as PCM in thermal energy storage in buildings: A review. *Renewable and Sustainable Energy Reviews* 15(3): 1675–1695.

Carbonaro C, Cascone Y, Fantucci S, et al. (2015) Energy assessment of a PCM – embedded plaster: Embodied energy versus operational energy. *Energy Procedia* 78: 3210–3215.

Cascone Y, Capozzoli A and Perino M (2018) Optimisation analysis of PCM-enhanced opaque building envelope components for the energy retrofitting of office buildings in Mediterranean climates. *Applied Energy* 211(July 2017): 929–953.

Castell A, Martorell I, Medrano M, et al. (2010) Experimental study of using PCM in brick constructive solutions for passive cooling. *Energy and Buildings* 42(4): 534–540.

Chang Y-H, Huang P-H, Wu BY, et al. (2015) A study on the color change benefits of sustainable green building materials. *Construction and Building Materials* 83: 1–6.

Clark WW, Atkinson Schaefer L, Wesley AK, et al. (2013) Variable thermal insulation. *US 2013/0081786 A1, United States*. Available at: https://patentimages.storage.googleapis.com/4c/2f/5b/03e3f3772a3019/US20130081786A1.pdf (accessed 5 August 2021).

Cui H and Overend M (2019) A review of heat transfer characteristics of switchable insulation technologies for thermally adaptive building envelopes. *Energy and Buildings* 199: 427–444.

Decreto-Lei n.º 251/2015 (2015) Portugal. Available at: https://dre.pt/application/conteudo/71100900 (accessed 5 August 2021).

Dimoudi A, Androutsopoulos A and Lykoudis S (2004) Experimental work on a linked, dynamic and ventilated, wall component. *Energy and Buildings* 36: 443–453.

Elsarrag E, Al-Horr Y and Imbabi MSE (2012) Improving building fabric energy efficiency in hot-humid climates using dynamic insulation. *Building Simulation* 5: 127–134.

EnergyPlus (2020) Available at: https://www.energyplus.net (accessed 11 November 2019).

EN ISO 6946:2007 (2007) Building components and building elements — Thermal resistance and thermal transmittance — Calculation method.

Fantucci S, Serra V and Perino M (2015) Dynamic insulation systems: Experimental analysis on a parietodynamic wall. *Energy Procedia* 78: 549–554.

Fateh A, Borelli D, Devia F, et al. (2018) Summer thermal performances of PCM-integrated insulation layers for light-weight building walls: Effect of orientation and melting point temperature. *Thermal Science and Engineering Progress* 6(December 2017): 361–369.

Fateh A, Borelli D, Spoladore A, et al. (2019) A state-space analysis of a single zone building considering solar radiation, internal radiation, and PCM effects. *Applied Sciences* 9(5): 832.

Favoino F, Jin Q and Overend M (2017) Design and control optimisation of adaptive insulation systems for office buildings. Part 1: Adaptive technologies and simulation framework. *Energy* 127: 301–309.

Favoino F, Loonen RCGM, Doya M, et al. (2018) *Building performance simulation and characterisation of adaptive facades – Adaptive facade network* (F Favoino, RCGM Loonen, M Doya, et al. eds). TU Delft open for the COST Action 1403 adaptive facade network editors. Available at: http://tu1403.eu/wp-content/uploads/Vol-3-2_for-web-Open-Access_9789463661119.pdf (accessed 5 August 2021).

Garshasbi S and Santamouris M (2019) Using advanced thermochromic technologies in the built environment: Recent development and potential to decrease the energy consumption and fight urban overheating. *Solar Energy Materials and Solar Cells* 191: 21–32.

Gassar AAA and Yun GY (2017) Energy saving potential of PCMs in buildings under future climate conditions. *Applied Sciences* 7(12): 1219.

Giancola E, Sanjuan C, Blanco E, et al. (2012) Experimental assessment and modelling of the performance of an open joint ventilated façade during actual operating conditions in Mediterranean climate. *Energy and Buildings* 54: 363–375.

Goia F, Chaudhary G and Fantucci S (2018) Modelling and experimental validation of an algorithm for simulation of hysteresis effects in phase change materials for building components. *Energy and Buildings* 174: 54–67.

Hu J and Yu XB (2019) Adaptive thermochromic roof system: Assessment of performance under different climates. *Energy and Buildings* 192: 1–14.

Ibañez-Puy M, Vidaurre-Arbizu M, Sacristán-Fernández JA, et al. (2017) Opaque ventilated façades: Thermal and energy performance review. *Renewable and Sustainable Energy Reviews* 79(April 2016): 180–191.

Imbabi MSE (2006) Modular breathing panels for energy efficient, healthy building construction. *Renewable Energy* 31(5): 729–738.

Isaia F, Fantucci S, Serra V, et al. (2019) The effect of airflow rate control on the performance of a fan-assisted solar air heating façade. *IOP Conference Series Materials Science and Engineering* 609(3): 1–6.

Izquierdo-Barrientos MA, Belmonte JF, Rodríguez-Sánchez D, et al. (2012) A numerical study of external building walls containing phase change materials (PCM). *Applied Thermal Engineering* 47: 73–85.

Jin Q, Favoino F and Overend M (2017) Design and control optimisation of adaptive insulation systems for office buildings. Part 2: A parametric study for a temperate climate. *Energy* 127(March): 634–649.

Juaristi M, Gómez-Acebo T and Monge-Barrio A (2018a) Qualitative analysis of promising materials and technologies for the design and evaluation of climate adaptive opaque façades. *Building and Environment* 144: 482–501.

Juaristi M, Monge-Barrio A, Sánchez-Ostiz A, et al. (2018b) Exploring the potential of smart and multifunctional materials in adaptive opaque facade systems. *Journal of Facade Design and Engineering* 6(2): 107–117.

Juaristi M, Loonen R, Isaia F, et al. (2020) Dynamic climate analysis for early design stages: A new methodological approach to detect preferable adaptive opaque façade responses. *Sustainable Cities and Society* 60: 102232.

Karlessi T, Santamouris M, Apostolakis K, et al. (2009) Development and testing of thermochromic coatings for buildings and urban structures. *Solar Energy* 83(4): 538–551.

Kimber M, Clark WW and Schaefer L (2014) Conceptual analysis and design of a partitioned multifunctional smart insulation. *Applied Energy* 114: 310–319.

Koenders SJ, Loonen RC and Hensen JL (2018) Investigating the potential of a closed-loop dynamic insulation system for opaque building elements. *Energy and Buildings* 173(173): 409–427.

Kuznik F, David D, Johannes K, et al. (2011) A review on phase change materials integrated in building walls. *Renewable and Sustainable Energy Reviews* 15(1): 379–391.

KIvasnin S (2014) Isolationsvorrichtung für Fenster oder Fassaden. DE 20 2014 000 533 U1, Germany. Available at: https://patentimages.storage.googleapis.com/3c/da/90/0903adce506adf/DE202014000533U1.pdf (accessed 17 September 2021).

Li ZX, Al-Rashed AAA, Rostamzadeh M, et al. (2019) Heat transfer reduction in buildings by embedding phase change material in multi-layer walls: Effects of repositioning, thermophysical properties and thickness of PCM. *Energy Conversion and Management* 195: 43–56.

Loonen RC, Singaravel S, Trčka M, et al. (2014) Simulation-based support for product development of innovative building envelope components. *Automation in Construction* 45: 86–95.

Loonen RC, Trčka M, Cóstola D, et al. (2013) Climate adaptive building shells: State-of-the-art and future challenges. *Renewable and Sustainable Energy Reviews* 25: 483–493.

Ministerio de Fomento (2019) Documento Básico HE Ahorro de Energía. *Código Téncico de la Edificación*: 1–129.

Ministry of Environment and Energy (2017) Thermophysical properties of structural materials and control of the temperature effect of the buildings. *Greece*. Available at: http://portal.tee.gr/portal/page/portal/SCIENTIFIC_WORK/GR_ENERGEIAS/kenak/files/TOTEE_20701-2_2017_TEE_1st_Edition.pdf (accessed 5 August 2021).

NCC Building Code of Australia (2019) Australia. Available at: https://build.com.au/bca-requirements-insulation (accessed 5 August 2021).

New Zealand Standards Executive (2009) Thermal insulation – Housing and small buildings. *New Zealand Standard*: 1–65. https://www.standards.govt.nz/shop/nzs-42182009/ (accessed 5 August 2021).

Park B and Krarti M (2016) Energy performance analysis of variable reflectivity envelope systems for commercial buildings. *Energy and Buildings* 124: 88–98.

Park B, Srubar WV and Krarti M (2015) Energy performance analysis of variable thermal resistance envelopes in residential buildings. *Energy and Buildings* 103: 317–325.

Peel MC, Finlayson BL and McMahon TA (2007) Updated world map of the Köppen-Geiger climate classification. *Hydrology and Earth System Sciences* 11: 1633–1644.

Peeters EAF and Dona MJ (2010) Device having adjustable heat-insulating properties. EP2233655B1, European Patent.

Perez G, Allegro VR, Corroto M, et al. (2018) Smart reversible thermochromic mortar for improvement of energy efficiency in buildings. *Construction and Building Materials* 186: 884–891.

Pflug T, Bueno B, Siroux M, et al. (2017) Potential analysis of a new removable insulation system. *Energy and Buildings* 154: 391–403.
Pflug T, Kuhn TE, Nörenberg R, et al. (2015) Closed translucent façade elements with switchable U-value—A novel option for energy management via the facade. *Energy and Buildings* 86: 66–73.
Sánchez MN, Giancola E, Suárez MJ, et al. (2017) Experimental evaluation of the airflow behaviour in horizontal and vertical open joint ventilated facades using stereo-PIV. *Renewable Energy* 109: 613–623.
Sunden B, Wu Z, Feng Z, et al. (2014) A comparative study on thermal conductivity and rheology properties of alumina and multi-walled carbon nanotube nanofluids. *Frontiers in Heat and Mass Transfer* 5: 1–10.
UCLA (2017) OPAQUE 3. Available at: https://opaque.software.informer.com/ (accessed 17 September 2021).
UNE-EN 16798-1 (2020) Energy performance of buildings ventilation for buildings.
Ürge-Vorsatz D, Cabeza LF, Serrano S, et al. (2015) Heating and cooling energy trends and drivers in buildings. *Renewable and Sustainable Energy Reviews* 41: 85–98.
Varga S, Oliveira AC and Afonso CF (2002) Characterisation of thermal diode panels for use in the cooling season in buildings. *Energy and Buildings* 34(3): 227–235.
Yılmaz Y and Yılmaz BÇ (2021) A weighted multi-objective optimisation approach to improve based facade aperture sizes in terms of energy, thermal comfort and daylight usage. *Journal of Building Physics* 44(5): 435–460.
Zheng S, Xu Y, Shen Q, et al. (2015) Preparation of thermochromic coatings and their energy saving analysis. *Solar Energy* 112: 263–271.

Appendix

Definition the static performance benchmark for each climate

Table A1. Analysed static opaque facades to identify the SPR for each location.

Facade typology	Possible claddings	Solar absorptance [-]	Admittance* (W/K)	Building materials	Acronym
Lightweight off-site wall (Figure 6(a) and (b))	White paint aluminium	0.30	2.33	EIFS finish + mineral wool* + plasterboard	1.Wh.lw
	Zink finishing	0.60			2.Zn.lw
	Matt black	0.90			3.Bl.lw
Medium-weight and heavyweight cavity wall (Figure 6(c))	Light colour brick	0.40	43.40	Brickwork outer leaf + mineral wool* + thermally improved hollow clay brick	4.Lbr.mw
	Dark colour brick	0.80			5.Dbr.mw
Heavyweight exposed concrete wall (Figure 6(d))	White paint	0.30	3435	Concrete cast dense + mineral wool*	6.Wh.hw
	Fair-faced concrete				7.Fc.hw
	Matt black	0.90			8.Bl.hw

*The total admittance of the façade was calculated for an insulation layer of mineral wool which had 0.16 m of thickness. The specific heat of each facade material is detailed in Table A4.

Table A2. Performance benchmark for each case study climate.

	Lisbon (PRT)	Athens (GRC)	Auckland (NZL)	Almeria (ESP)	Tenerife (ESP)	Brisbane (AUS)
U value (W/m^2 K)	0.40 (Decreto-Lei n.º 251/, 2015)	0.45 (Ministry of Environment and Energy, 2017)	0.34 (New Zealand Standards Executive, 2009)	0.44 (Ministerio de Fomento, 2019)	0.56 (Ministerio de Fomento, 2019)	0.36 (NCC Building Code of Australia, 2019)

[*]The *U*-value applied to each static opaque façade configuration was the one recommended or required by the national regulation of each country. The thickness of the mineral wool was calculated accordingly.

Table A3. Static performance benchmark for each case study climate.

Climate	SPR	U value (W/m^2 K)	DE (kWh/m^2)	HE (kWh/m^2)	CE (kWh/m^2)
Lisbon (PRT)	6.Wh.hw	0.40	4.80	1.59	14.57
Athens (GRC)	6.Wh.hw	0.45	7.17	3.59	20.07
Auckland (NZL)	6.Wh.hw	0.34	2.12	2.19	4.38
Almeria (ESP)	6.Wh.hw	0.44	5.50	0.44	18.63
Tenerife (ESP)	6.Wh.hw	0.56	7.17	0	25.10
Brisbane (AUS)	6.Wh.hw	0.36	5.39	0	18.86

Properties of simulated façade materials

Table A4. Thermal properties of static façade materials.

Material	Thickness (m)	Conductivity (W/m K)	Density (kg/m^3)	Specific heat (J/kg K)	Roughness
Mortar	0.001	0.7	1100	900	Medium smooth
Mineral wool (MW)	According to U ref	0.04	25	1000	Medium rough
Brickwork outer leaf	0.115	0.84	1700	800	Medium smooth
Concrete cast dense exterior	0.25	1.4	2100	840	Medium smooth
Concrete cast Dense interior	0.20	1.9	2300	840	Medium smooth
Thermally improved hollow clay brick	0.29	0.24	800	800	Medium smooth
Plasterboard	0.012	0.16	950	840	Smooth
Cross laminated timber (CLT)	0.12	0.13	450	1600	Smooth

Table A5. Thermal properties of static façade finishing materials.

Material	Thermal resistance (m^2 K/W)	Thermal absorptance	Solar absorptance	Roughness
White paint	0.92	0.3	0.3	Medium smooth
Zink finishing	0.9	0.6	0.6	Medium smooth
Matt black	0.96	0.96	0.96	Medium smooth
Light colour brick	0.9	0.4	0.4	Medium smooth
Dark colour brick	0.9	0.8	0.8	Medium smooth
Aluminium	0.3	0.3	0.3	Smooth

Table A6. Window design parameters.

Design parameters of double-glazing unit	
U-value (W/m^2 K)	1.4
Solar heat gain coefficient	0.55
Visible transmittance	0.74
Shadow system	Blind with low reflectivity slats in the exterior side of the window. Min slat angle 180°, Max slat angle 45° Control: cut-off solar radiation according to the external air temperature ($T > 24$°C)

Table A7. Thermal properties of static building materials.

Building component	Material	Thickness (m)	Conductivity (W/m K)	Density (kg/m^3)	Specific heat (J/kg K)	Roughness	T hermal resistance (m^2 K/W)
Interior partition (Layer 1 and 3)	Gypsum plasterboard	0.0158	0.25	900	1000	Rough	–
Interior partition (Layer 2)	Insulation layer	–	–	–	–	–	0.15
Slab (Layer 1)	Cast concrete	0.3	1.4	2100	840	Rough	
Slab (Layer 2)	Air gap	0.015	–	–	–	–	0.57
Slab (Layer 3)	Floor tile	0.019	0.55	273.7	712	Rough	–

Table A8. Simulated facade configurations for hw and lw facade options.

Typology	Layer 1	Layer 2	Layer 3	Layer 4	Layer 5	Layer * Lw
b.TCH.1	TCH coating	Ext. concrete	MW	Int. concrete*	–	Plasterboard
b.TCH.2	TCH coating	Brickwork	Closed air cavity	AIS	Thermally improved brick	–
b.TCH.3	TCH coating	Mortar	Air cavity	MW	Int. concrete*	Plasterboard
a.AC.3	White mortar	Air cavity	MW	Int. concrete*	–	Plasterboard
b.KC.1	KC	Mortar	MW	Int. concrete*	–	Plasterboard
c.AIS.1	White mortar	AIS	Concrete*	–	–	CLT
c.AIS.2	Brickwork	Closed air cavity	AIS	Thermally improved brick	–	–
c.AIS.3	White mortar	Air cavity	AIS	Int. concrete*	–	CLT
b.TCH + c.AIS.1	TCH mortar	AIS	Concrete*	–	–	CLT
b.TCH + c.AIS.2	TCH coating	Brickwork	Closed air cavity	MW	Plasterboard	–
b.TCH + c.AIS.3	TCH mortar	Air cavity	AIS	Int. concrete*	–	CLT
a.AC + b.TCH.3	TCH mortar	Air cavity	MW	Int. concrete*	–	Plasterboard
b.KC + c.AIS.1	White mortar	AIS	Concrete*	–	–	CLT
a.AC + b.KC.3	KC	Mortar	Air cavity	MW	Int. concrete*	Plasterboard
a.AC + b.KC + c.AIS.3	KC	Mortar	Air cavity	AIS	Int. concrete*	CLT

*Layer to be substituted when mw/lw configurations are evaluated.

EMS details for each AOF typology

Table A9 summarizes the sensors and the algorithms which are needed to define the adaptive behaviour of each facade typology. For some AOF typologies, the sensor can be placed either in the outside and inside face of the AOF system or in the outside and inside face of AIS. The decision was based on the IDE, by comparing the results of the simulation models which sensors are placed in the interior layer of the AOF (int) and in the inner layer of Adaptive Insulation (AIS). The decisions about the sensor's placement for each AOF typology and climate are summarized in Table A10.

The control logic used in this research were rule-based and the EMS programs applied for each AOF typology are available as Supplementary Material.

Table A9. Sensors and algorithms used within EMS to model when the adaptive response happens according to the measured physical parameters.

Energy management system class list	Measured physical parameter	Actuated element			
		TCH	CA	AC	AIS
Sensor	Surface outside face temperature	x	x		x
	Surface inside face temperature		x*		x*
	Surface temperature of the exterior surface of the AIS				x*
	Surface temperature of the interior surface of the AIS		x*		x*
	Zone air system sensible heating energy		x	x	x
	Zone air system sensible cooling energy		x	x	x
	Site wind speed			x	
Global variable	Average surface outside face temperature of the last 48 h**		x	x	x

*For some AOF typologies, the sensor can be placed either in the outside and inside face of the AOF system or in the outside and inside face of AIS.

When there is no heating or cooling demand, average surface outside face temperature of the last 48 h was used to assume if it was a heating or cooling demand period.

Table A10. Final decision on the sensor's placement for each AOF typology and climate.

Climate	c.AIS.1	c.AIS.2	c.AIS.3	b.TCH + c.AIS.1	b.TCH + c.AIS.2	b.TCH + c.AIS.3	b.KC + c.AIS.1	a.AC + b.KC.3	a.AC + b.KC + c.AIS.3
Lisbon (PRT)	int*	AIS	AIS	–	AIS	AIS	AIS	–	AIS
Athens (GRC)	int*	AIS	AIS	–	AIS	AIS	AIS	–	AIS
Auckland (NZL)	AIS	AIS*	AIS	–	AIS*	AIS	AIS*	–	AIS*
Almeria (ESP)	AIS	AIS	AIS	–	AIS	AIS	AIS*	–	AIS
Tenerife (ESP)	int*	–	AIS	–	–	AIS	AIS	–	AIS
Brisbane (AUS)	int	AIS	int	int	AIS	int	Int	–	AIS*

*When both options had similar IDE.

Detailed simulation outputs

Table A11. Total Annual Delivered Energy (DE), Heating Energy use (HE) and Cooling Energy use (CE) (kWh/m^2) for 15 AOF typologies with different thermal mass.

			Complexity Level 1			Complexity Level 2					Complexity Level 3				Complexity Level 4		
			b.TCH.1	b.TCH.2	b.TCH.3	a.AC.3	b.KC.1	c.AIS.1	c.AIS.2	c.AIS.3	b.TCH + c.AIS.1	b.TCH + c.AIS.2	b.TCH + c.AIS.3	a.AC + b.TCH.3	b.KC + c.AIS.1	a.AC + b.KC.3	a.AC + b.KC + c.AIS.3
Lisbon	HE	hw/mw	1.52	1.86	1.50	1.54	1.36	1.06	1.02	1.05	1.16	1.01	0.94	1.48	0.66	1.83	0.84
		lw	1.72	–	1.67	1.71	1.57	1.05	–	1.05	1.14	–	0.95	1.65	0.72	2.00	0.95
	CE	hw/mw	14.75	14.92	14.87	14.75	15.33	13.22	14.86	13.39	15.58	14.64	13.58	14.94	11.82	15.82	11.72
		lw	15.36	–	15.40	15.26	15.49	14.05	–	14.21	15.75	–	14.35	15.47	13.18	16.43	13.48
	DE	hw/mw	4.82	5.01	4.85	4.83	4.92	4.20	4.65	4.25	4.91	4.59	4.25	4.86	3.64	5.25	3.68
		lw	5.08	–	5.07	5.04	5.05	4.43	–	4.48	4.96	–	4.48	5.08	4.05	5.49	4.23

(continued)

Table A11. Continued

			Complexity Level 1			Complexity Level 2					Complexity Level 3				Complexity Level 4		
			b.TCH.1	b.TCH.2	b.TCH.3	a.AC.3	b.KC.1	c.AIS.1	c.AIS.2	c.AIS.3	b.TCH + c.AIS.1	b.TCH + c.AIS.2	b.TCH + c.AIS.3	a.AC + b.TCH.3	b.KC + c.AIS.1	a.AC + b.KC.3	a.AC + b.KC + c.AIS.3
Athens	HE	hw/mw	3.46	3.98	3.43	3.50	3.13	2.43	2.35	2.43	2.64	2.33	2.20	3.38	1.62	4.04	1.97
		lw	3.70	–	3.61	3.67	3.39	2.39	–	2.40	2.57	–	2.20	3.56	1.73	4.21	2.18
	CE	hw/mw	20.01	20.30	20.03	20.10	21.03	18.10	19.89	18.34	22.16	19.53	18.26	20.08	16.64	21.21	16.72
		lw	20.42	–	20.44	20.49	20.94	18.66	–	18.88	21.37	–	18.82	20.49	17.80	21.71	18.25
	DE	hw/mw	7.10	7.39	7.09	7.14	7.26	6.14	6.62	6.21	7.39	6.51	6.10	7.09	5.40	7.68	5.57
		lw	7.32	–	7.28	7.32	7.34	6.29	–	6.35	7.13	–	6.26	7.28	5.78	7.89	6.09
Auckland	HE	hw/mw	2.12	2.46	2.08	2.12	1.95	1.63	1.44	1.60	1.67	1.43	1.48	2.06	1.20	2.47	1.49
		lw	2.28	–	2.22	2.25	2.12	1.55	–	1.54	1.60	–	1.43	2.19	1.20	2.60	1.52
	CE	hw/mw	4.60	4.64	4.69	4.51	4.69	3.86	4.50	3.95	4.06	4.55	4.20	4.73	3.21	4.76	3.08
		lw	5.06	–	5.11	4.89	4.87	4.55	–	4.64	4.76	–	4.84	5.15	4.13	5.22	4.16
	DE	hw/mw	2.16	2.31	2.17	2.14	2.12	1.75	1.86	1.77	1.83	1.87	1.79	2.18	1.40	2.35	1.48
		lw	2.36	–	2.35	2.30	2.24	1.92	–	1.94	2.00	–	1.96	2.35	1.66	2.53	1.80
Almeria	HE	hw/mw	0.39	0.66	0.40	0.43	0.28	0.14	0.17	0.15	0.23	0.17	0.09	0.39	0.01	0.59	0.04
		lw	0.62	–	0.59	0.61	0.50	0.17	–	0.17	0.25	–	0.12	0.57	0.04	0.80	0.09
	CE	hw/mw	18.73	18.90	18.82	18.71	19.42	16.54	18.81	16.87	19.61	18.51	16.89	18.84	14.61	19.69	14.69
		lw	19.23	–	19.30	19.16	19.42	17.47	–	17.76	19.63	–	17.77	19.32	16.36	20.27	16.92
	DE	hw/mw	5.51	5.66	5.54	5.52	5.66	4.78	5.44	4.88	5.69	5.36	4.86	5.54	4.18	5.86	4.21
		lw	5.74	–	5.75	5.72	5.75	5.06	–	5.14	5.71	–	5.13	5.75	4.69	6.11	4.87
Tenerife	HE	hw/mw	0.00	0.00	0.00	0.00	0.00	0.00	0.00	0.00	0.00	0.00	0.00	0.00	0.00	0.00	0.00
		lw	0.00	0.00	0.00	0.00	0.00	0.00	0.00	0.00	0.00	0.00	0.00	0.00	0.00	0.00	0.00
	CE	hw/mw	25.43	25.19	25.67	25.37	25.75	22.27	25.88	22.65	25.49	25.59	22.76	25.76	18.88	27.49	18.99
		lw	26.11	–	26.25	25.91	25.76	24.01	–	24.36	26.44	–	24.42	26.35	21.90	28.27	22.97
	DE	hw/mw	7.27	7.20	7.33	7.25	7.36	6.36	7.40	6.47	7.28	7.31	6.50	7.36	5.39	7.86	5.43
		lw	7.46	–	7.50	7.40	7.36	6.86	–	6.96	7.56	–	6.98	7.53	6.26	8.08	6.56
Brisbane	HE	hw/mw	0.00	0.00	0.00	0.00	0.00	0.00	0.00	0.00	0.00	0.00	0.00	0.00	0.00	0.00	0.00
		lw	0.00	0.00	0.00	0.00	0.00	0.00	0.00	0.00	0.00	0.00	0.00	0.00	0.00	0.00	0.00
	CE	hw/mw	18.91	19.07	19.03	18.96	19.83	16.49	19.15	16.91	19.72	18.67	16.91	19.04	14.19	20.49	14.29
		lw	19.55	–	19.65	19.56	19.71	17.61	–	17.94	20.02	–	17.95	19.66	16.31	21.26	16.93
	DE	hw/mw	5.40	5.45	5.44	5.42	5.67	4.71	5.47	4.83	5.64	5.33	4.83	5.44	4.05	5.86	4.08
		lw	5.59	–	5.61	5.59	5.63	5.03	–	5.13	5.72	–	5.13	5.62	4.66	6.08	4.84

Table A12. IHE, ICE and IDE [%] to check if SPR is improved or not by 15 AOF typologies with different thermal mass.

			Complexity Level 1			Complexity Level 2					Complexity Level 3				Complexity Level 4		
			b.TCH.1	b.TCH.2	b.TCH.3	a.AC.3	b.KC.1	c.AIS.1	c.AIS.2	c.AIS.3	b.TCH + c.AIS.1	b.TCH + c.AIS.2	b.TCH + c.AIS.3	a.AC + b.TCH.3	b.KC + c.AIS.1	a.AC + b.KC.3	a.AC + b.KC + c.AIS.3
Lisbon	IHE	hw/mw	4.30	−17.08	5.22	2.73	14.52	33.43	35.76	33.71	27.21	36.60	41.06	6.59	58.57	−15.44	47.22
		lw	−8.50	–	−5.27	−7.61	1.31	34.08	–	34.05	28.00	–	40.22	−3.98	54.75	−26.10	40.15
	ICE	hw/mw	−1.24	−2.44	−2.04	−1.23	−5.26	9.28	−1.97	8.09	−6.94	−0.49	6.81	−2.54	18.90	−8.62	19.57
		lw	−5.43	–	−5.71	−4.72	−6.31	3.58	–	2.49	−8.09	–	1.48	−6.21	9.51	−12.75	7.48
	IDE	hw/mw	−0.51	−4.38	−1.08	−0.70	−2.64	12.47	3.02	11.48	−2.42	4.42	11.35	−1.33	24.15	−9.52	23.23
		lw	−5.83	–	−5.65	−5.10	−5.30	7.62	–	6.67	−3.31	–	6.61	−5.91	15.50	−14.52	11.81
Athens	IHE	hw/mw	3.45	−11.00	4.42	2.53	12.69	32.20	34.41	32.13	26.46	35.05	38.75	5.80	54.95	−12.69	45.10
		lw	−3.14	–	−0.64	−2.43	5.39	33.37	–	33.13	28.23	–	38.68	0.64	51.76	−17.41	39.12
	ICE	hw/mw	0.31	−1.16	0.19	−0.14	−4.78	9.82	0.89	8.62	−10.43	2.71	9.02	−0.03	17.08	−5.69	16.67
		lw	−1.76	–	−1.84	−2.10	−4.33	7.05	–	5.95	−6.46	–	6.24	−2.09	11.31	−8.16	9.09
	IDE	hw/mw	0.94	−3.13	1.04	0.40	−1.28	14.30	7.60	13.32	−3.05	9.18	14.97	1.14	24.66	−7.09	22.36
		lw	−2.04	–	−1.60	−2.17	−2.38	12.32	–	11.39	0.48	–	12.73	−1.54	19.40	−10.02	15.10
Auckland	IHE	hw/mw	3.18	−12.47	4.66	2.80	10.85	25.65	33.95	26.59	23.46	34.69	32.07	5.84	45.13	−13.18	31.94
		lw	−4.17	–	−1.40	−3.07	3.07	29.14	–	29.65	26.71	–	34.40	−0.25	45.32	−19.05	30.62
	ICE	hw/mw	−4.99	−5.93	−7.20	−2.92	−7.03	11.74	−2.72	9.70	7.29	−4.02	4.09	−8.10	26.61	−8.63	29.54
		lw	−15.65	–	−16.74	−11.61	−11.24	−3.98	–	−6.00	−8.79	–	−10.60	−17.60	5.74	−19.15	4.87
	IDE	hw/mw	−1.63	−8.62	−2.32	−2.92	0.33	17.47	12.37	16.65	13.94	11.91	15.60	−2.36	34.23	−10.50	30.53
		lw	−10.93	–	−10.43	−8.10	−5.35	9.64	–	8.67	5.81	–	7.91	−10.46	22.02	−19.11	15.46
Almeria	IHE	hw/mw	9.69	−50.15	8.11	1.97	35.90	67.17	60.56	66.33	48.09	61.56	78.38	11.53	96.87	−36.29	91.54
		lw	−42.65	–	−35.28	−40.12	−14.10	62.10	–	61.00	43.36	–	71.66	−31.66	91.38	−84.21	79.24
	ICE	hw/mw	−0.54	−1.44	−1.02	−0.40	−4.20	11.23	−0.93	9.48	−5.26	0.67	9.33	−1.10	21.57	−5.69	21.19
		lw	−3.22	–	−3.58	−2.85	−4.20	6.24	–	4.71	−5.35	–	4.64	−3.69	12.19	−8.80	9.20
	IDE	hw/mw	−0.21	−2.98	−0.73	−0.33	−2.93	13.01	1.02	11.28	−3.57	2.60	11.53	−0.70	23.96	−6.66	23.42
		lw	−4.47	–	−4.59	−4.03	−4.52	8.02	–	6.50	−3.80	–	6.76	−4.57	14.71	−11.20	11.43
Tenerife	IHE	hw/mw	–	–	–	–	–	–	–	–	–	–	–	–	–	–	–
		lw	–	–	–	–	–	–	–	–	–	–	–	–	–	–	–
	ICE	hw/mw	−1.29	−0.36	−2.26	−1.05	−2.55	11.30	−3.10	9.76	−1.52	−1.93	9.36	−2.59	24.80	−9.52	24.35
		lw	−4.01	–	−4.57	−3.22	−2.61	4.37	–	2.95	−5.34	–	2.72	−4.95	12.78	−12.61	8.49
	IDE	hw/mw	−1.29	−0.36	−2.26	−1.05	−2.55	11.30	−3.10	9.76	−1.52	−1.93	9.36	−2.59	24.80	−9.52	24.35
		lw	−4.01	–	−4.57	−3.22	−2.61	4.37	–	2.95	−5.34	–	2.72	−4.95	12.78	−12.61	8.49

(continued)

Table A12. Continued

			Complexity Level 1			Complexity Level 2					Complexity Level 3				Complexity Level 4		
			b.TCH.1	b.TCH.2	b.TCH.3	a.AC.3	b.KC.1	c.AIS.1	c.AIS.2	c.AIS.3	b.TCH + c.AIS.1	b.TCH + c.AIS.2	b.TCH + c.AIS.3	a.AC + b.TCH.3	b.KC + c.AIS.1	a.AC + b.KC.3	a.AC + b.KC + c.AIS.3
Brisbane	IHE	hw/mw	–	–	–	–	–	–	–	–	–	–	–	–	–	–	–
		lw	–	–	–	–	–	–	–	–	–	–	–	–	–	–	–
	ICE	hw/mw	–0.25	–1.14	–0.89	–0.51	–5.14	12.58	5.47	10.32	–4.58	5.33	10.35	–0.97	24.75	–8.67	24.21
		lw	–3.68	–	–4.19	–3.71	–4.53	6.63	–	4.85	–6.18	–	4.80	–4.27	13.52	–12.77	10.24
	IDE	hw/mw	–0.25	–1.14	–0.89	–0.51	–5.14	12.58	5.47	10.32	–4.58	5.33	10.35	–0.97	24.75	–8.67	24.21
		lw	–3.68	–	–4.19	–3.71	–4.53	6.63	–	4.85	–6.18	–	4.80	–4.27	13.52	–12.77	10.24